

**Response to Anonymous Referees,**

***“Cloud Characteristics, Thermodynamic Controls and Radiative Impacts During the Observations and Modeling of the Green Ocean Amazon (GoAmazon2014/5) Experiment”***

5

**Scott E. Giangrande et al.**

10 The authors would like to thank all reviewers for their helpful comments and suggestions. We have responded to all reviewers in a single document, since several comments are similar. As a brief summary, the revisions to the manuscript include the following highlights:

- 15 • We have modified several of the previous images (fonts, lines, sizing, etc.) and added a few new / revised plots that combine image ideas.
- The manuscript has incorporated several changes in response to reviewer comments on uncertainty/representativeness. Specifically, we have included a new image and discussion section (in Section 3) in response to the representativeness of these observations as compared to satellite-based platform references (MODIS, GOES) – Reviewer 3; This also is one practical way to approach some of the observational uncertainty concerns from Reviewer 1.
- 20 • We have attempted to clarify the text on the convective/stratiform precipitation and how this regime segregation is related to the cloud classification – We note, this separation is different than ‘deep convective’ cloud regime classifications, in that these deep convective regimes may contain convective and stratiform precipitation components.
- 25 • We have included a ‘Data Availability’ section, as required by the journal.

The individual reviewer comments and responses are included in the following document (author comments in **bold**, reviewer comments in *italics*).

30

35

## Response to Anonymous Referee #1

5 *This manuscript summarizes observational data collected during the GoAmazon campaign, emphasizing on cloud/precipitation-related properties, the dry-vs-wet season contrast, as well as diurnal variation. As the first field campaign in tropical rainforest region so comprehensive, I think the results presented here are interesting, and will be useful to the community. Overall the manuscript is well-written, and I look forward to seeing this manuscript published on ACP. I do have four general comments that the authors could consider, and would, in my opinion, make the manuscript more accessible and useful to readers, especially those from modeling side.*

10 **We thank the reviewer for their kind words and we hope our revisions are sufficient to address many concerns of this reviewer.**

*General comments:*

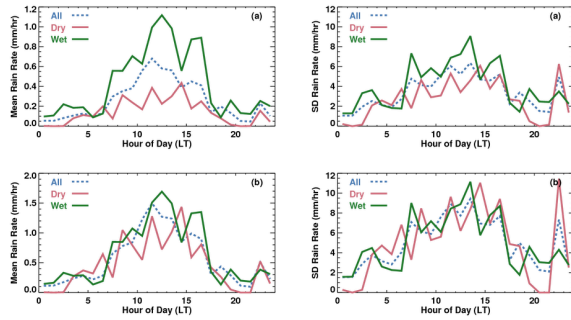
15 *First, proxies of uncertainty/variability (e.g., standard error, standard variation, or interquartile range) could be added to Figure 7 and Table 2 (and Table 3 if the authors have the necessary data). While Table 2 has been visualized, with some variation/extension, in Figures 10 and 11, an additional figure with values listed in Table 2 plus uncertainty/variability could make the results easier to digest.*

20 **This is a very good comment, but difficult to answer. These observations are challenging to bound as they merge several ARM observations to maximize designation of clouds. Another concern when addressing this comment is that in some instances, the suggested ‘proxy’ ways to report spread (standard deviation) may add confusion (e.g., it is not trivial to explain what those values represent).**

25 **To begin, there are not many independent observations to act as reference for cloud frequency (esp. under all cloud conditions reported). In our response to Reviewer 3, we added to Section 3 a comparison with independent passive satellite observations (MODIS, GOES) for Shallow Cumulus; Note, even this approach implies new complexities (interpretation) because those cloud sampling techniques are different. Yet, this is one way to address sampling/representativeness concerns, as well as to gauge the uncertainty of T3 cloud observations (existing reference).**

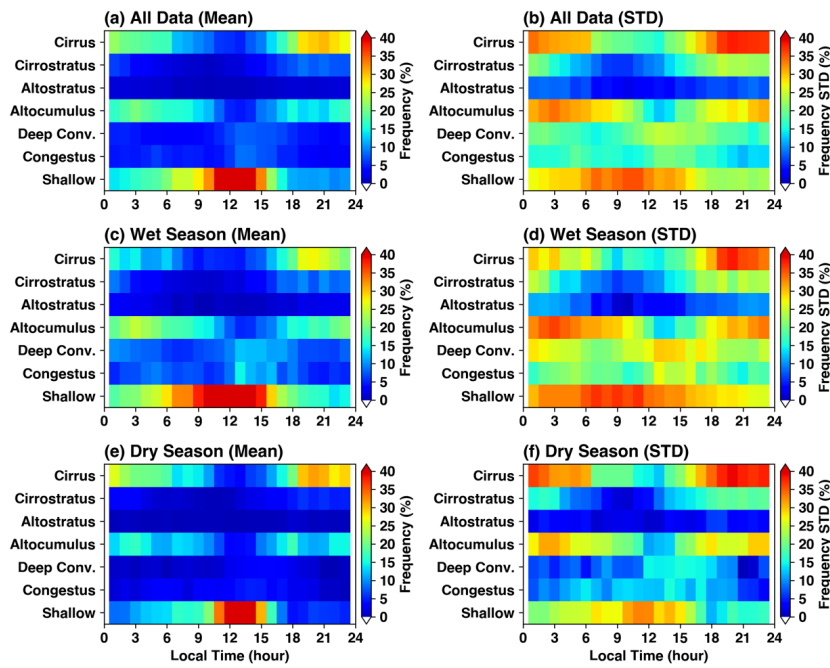
30 **Second, given the large diurnal variability and the nature of the instantaneous observations, the authors suggest it may not always make sense to condense what is reported by Tables 2 or 3 (or Figure 7) down to a single value (e.g., reporting a single standard deviation). One example for this reviewer is specific to Figure 7, but a case where we believe the application falls short of the anticipated outcome. Below, we plot the standard deviations for Figure 7ab, noting that these values are substantially larger than the mean rainfall rates (would require also a significant re-**

plotting). Now, this is not a surprising result, given that these are ‘instantaneous’ (5-minute) rainfall rate measurements as compared to a mean value for a given hourly interval:



Here, it would not be difficult to include these references to our revised manuscript; However, we question the value for presenting this as ‘uncertainty’, inasmuch that the instantaneous values used to estimate those standard deviations also reflect the many contributions from zero value data points, etc.; Rather, we have included the total accumulation plot (new Figure 7c), which should help impress that the number/probability for observing surface rainfall during certain hours are substantially lower.

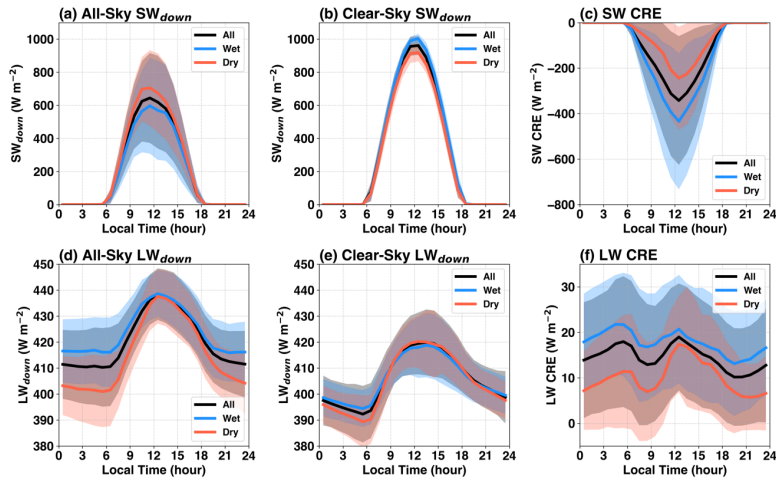
- 10 Similarly, the variability of cloud frequency and CREs reported in Table 2 are difficult to be condensed into a single number. Because of the nature of a point measurement, occurrence of cloud at any given instance is either 1 or 0, the standard deviation for the same hour across different days are oftentimes as large as, or exceed, the mean value (see figure below). This is true for most of the cloud types except shallow cumulus during the middle of the day. In addition, the standard deviations themselves have a large diurnal variability. Therefore, the authors believe it does not make sense to report a single standard deviation (or similar quantity representing variability) number for each of the cloud type in Table 2. The only variable that does not have a strong diurnal variability is SW Transmissivity.
- 15
- 20 Thus, to respond to the Reviewer we added the standard deviations of SW transmissivity calculated across the diurnal cycle to Table 2.



Mean (left column) and standard deviation (right column) of cloud frequency of occurrence as the lowest cloud in the column for (a,b) all data, (c,d) wet season, (e,f) dry season.

5 In the case of Table 3 and its associated discussion, we agree that more information could be valuable in this application. In this case, we have included a new figure into the revised Section 4 that helps demonstrate the full diurnal cycle of variables in Table 3, as shown below. Here, the hourly standard deviation is represented by the shaded regions.

10



New Figure added to complement Table 3.

Second, some analysis of TRMM 3B42 data have shown that the diurnal cycle at/around the GoAmazon site is rather unique compared with other tropical locations over land because the precipitation at the site peaks around noon instead of late afternoon (*author snip to save space*)... I think it would be helpful if the authors could, to the best of their current knowledge, and with the dry-vs-wet season contrast at the GoAmazon site in mind, add a short paragraph or two to comment on the uniqueness of the GoAmazon site (*i.e.*, whether the diurnal cycle at this site is really different from other sites) and, if this site is indeed unique, to synthesize the similarities and differences of the precipitation/CF diurnal cycle at the GoAmazon site compared with other tropical locations over land (*e.g.*, the larger Amazon basin, and/or Congo basin and maritime continent).

One important addition to this manuscript is the comparison against available satellite ShCu observations that may also help demonstrate spatial representativeness in a manner not previously covered by other authors.

This topic (representativeness) was the focus of a related GoAmazon2014/5 effort by some of our coauthors – Burleyson et al. 2016 (JAMC). Their primary finding was that the diurnal cycle of deep convection around the GoAmazon sites is a superposition of locally forced convection and the inland propagation of the previous day's sea-breeze front. Their climatology showed that deep convection begins around noon around the sites, and has a broad peak in the mid-afternoon over

the T3 site. There is also some variability among the various GoAmazon2014/5 sites that is related to localized circulations generated by the river breezes.

5 More to the Reviewer's original comment, the diurnal cycle at the T3 site is generally well correlated with the regional behaviors to within a few degrees of the site; We note that the correlation drops off sharply at distances more than a few hundred kilometers, and this is particularly important during the wet season. We would encourage the reviewers (or those reading these response) to download that paper for more information.

10 Here, we also include the following references to the Burleyson et al. study that were in our original and revised versions of the manuscript:

15 P3, L17-20: "Seasonal thermodynamical shifts, as well as additional large-scale sea-breeze front type intrusions into the basin (e.g., Cohen et al. [1995], Alcântara et al. [2011]), promote additional cloud lifecycle complexity and diurnal cycle of precipitation variability (e.g., Burleyson et al. [2016], Saraiva et al. [2016])."

20 P9, L17-20: "The T3 location exhibits a pronounced diurnal cycle associated with deeper convection (as also in Saraiva et al. [2016]). This pronounced behavior is further representative of the fortuitous placement for the T3 AMF site, wherein daily cloud lifecycles also phase well with propagating sea breeze intrusions over this portion of the Amazon basin [Burleyson et al. 2016]."

25 P11, L1-5: "Overnight and/or pre-dawn deep convection (e.g., organized, continuation) and additional local congestus development are more common in the wet season. The distinct nighttime enhancement in stratiform precipitation (identified as "Deep Convection" in Figs. 6d, 8d and 9d) during the wet season is consistent with previous findings that propagating convective cloud systems contribute to the observed diurnal cycle of deep convection [e.g., Burleyson et al. 2016, Tang et al. 2016]."

30 *Third, partitioning precipitation (e.g., into convective vs stratiform precipitation) can be tricky, and the way adopted by different parameterizations differ. In some cases, C2 it may be difficult (if not impossible) to draw an analogy between observation and a parameterization. Therefore, it would be helpful if the authors could add a line or two to give some details regarding the definition of convective and stratiform rain (I thought the former is defined as all precipitation associated with*  
35 *shallow, congestus, deep convective, and altocumulus, but this would be inconsistent with the description in p11, l. 3: '... stratiform precipitation (identified as "Deep Convection" in ... ' which is not obvious to me since bright band is not used as a criterion for the cloud-type algorithm...'). Furthermore, given the potential issue of precipitation partitioning, precipitation rate conditioned on different cloud types could eventually be even more valuable for modeling groups (e.g., add an additional figure like Figure 11, but for precipitation rate; this last suggestion is totally optional for the authors).*

**We have attempted to improve discussion on this subject. We agree that it may be confusing to readers that a single category of ‘deep convective’ clouds is associated with ‘convective’ and ‘stratiform’ rain components.**

5 *Fourth, both Figures 10 and 11 seem to put more emphasis on SW than LW. Both SW and LW are important for quantifying local energy budget, and some recent modeling studies have demonstrated that LW could impact the development and maintenance of organized system, which has been documented by Bu et al. 2017 (The influences of boundary layer mixing and cloud-radiative forcing on tropical cyclone size. JAS), and the LW feedback is essential to convective self-aggregation under certain conditions, which has been summarized in Wing et al. 2017 (Convective self-aggregation in numerical simulations: a review. Surv. Geophys. Sec. 3.2). Given this increasing interests in LW-related processes, the authors could consider to add additional LW information to Figures 10 and 11.*

15 **The LW feedbacks that previous studies and this Reviewer discuss are related to the LW cloud radiative heating profile (contributions from cloud and water vapor) in the atmosphere. This is different from the definition used in our study for "surface cloud radiative effects" (e.g., this is the explanation why Fig. 10c LW CRE is an order of magnitude smaller than SW CRE).**

Specific comments:

20 p3, l. 13: "...unique precipitation cycles as compared to the conditions over the larger Amazon basin". Please see my second general comment.

**As in response to the general comment.**

25 p3, l. 24: "environmental forcing datasets" could be more specific.

**Revised to "Large-scale forcing datasets (including advective tendencies and vertical velocities) over this region were also supported by ..."**

30 p4, l. 7: "a cloud-type classification algorithm" refers to Table 1?

**Yes. This refers to the cloud classification algorithm performed on the combined RWP+ARSCL datasets that is partially summarized by Table 1, and for example also feeds into the calculations for Table 2, etc.**

p4, l. 27: "Figure 2...average daily profile..." it would be nice if the original temporal frequencies of the raw data can be mentioned here (from p. 8, l. 17, hourly profile estimates are used).

5 **It is unclear if this action is necessary / the authors are unsure how to respond - certain measurements in this figure are obtained at higher frequency than others (aka, between radiosondes versus radar, etc.), across the various plots. The ARM raw data sampling is more frequent than hourly for many instruments (typically seconds to minutes in the case of radar and/or gauge sampling), as noted in the associated instrument sections.**

10 p5, l. 2: "CAPE, CIN and ...and heightened moisture." Figure 3 (not 2) shows that CIN behaves differently in wet vs dry seasons, but not so much for CAPE. But in any event, the behavior of CAPE and CIN described here is not clear from Figure 2.

15 **Figure 2 shows the time series of CAPE and CIN. As also raised by other reviewers, we agree with this reviewer that it is difficult to view pronounced changes in these variables related to the separate wet and dry season intervals. We would agree this is easier to suggest these variations in terms of Figure 3 or dataset median values; For example, Figure 3 we believe does suggest that CAPE is higher during the dry season (especially at midday), and CIN is also greater (more negative) during the dry season. However, we have attempted to clarify what the ARM observations demonstrate in our manuscript (as compared to those observations of others).**

20 p5, l. 22: "increased CIN" in terms of magnitude, regardless of its sign?

**Agree. We now mention this refers to the absolute values of CIN.**

25 p5, l. 26: "total advection...of moisture". I assume that this means  $-u \cdot \nabla q$  instead of  $u \cdot \nabla q$ .

**Yes. We revised the text to add the equations:**

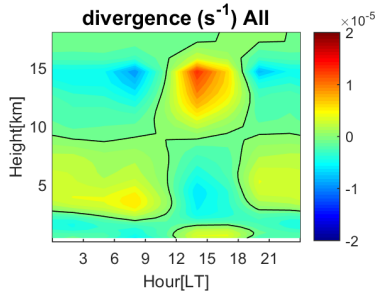
**"Fig. 4 plots the diurnal cycle of the large-scale vertical motion (omega), total advection of moisture and relative humidity. The total advection of moisture is the sum of the horizontal and the vertical advectons:**

30 
$$q\_adv\_t = -V_h \cdot \nabla_h q - \omega \frac{\partial q}{\partial p} "$$

p5, l. 33: “The evening and early morning hours exhibit upward air motion confined below 3-4 km”. How should we interpret this feature? For instance, based on the first law of thermodynamics, we have  $\omega = pQ/cvT - \gamma p \nabla \cdot u$ , where  $Q$  represents the diabatic heating/cooling rate. Can we explain the feature by low-level radiative cooling?

5 **We suggest that the vertical velocity feature can be explained by the low-level convergence and middle-level divergence in the evening and early morning (see the figure below). This may be related to the congestus clouds during this period. We have revised the text to add an interpretation of this feature:**

10 *“The evening and early morning hours exhibit upward air motion confined below 3-4 km, due to the lower-level convergence and middle-level divergence (not shown), likely corresponding to the congestus clouds.”*



p6, l. 2: “positive advection of moisture” means  $-u \cdot \nabla q > 0$ ? (and p9, l. 8.)

15 **Yes.**

p6, l. 2: “Between 4-8 km ... (Fig. 4g).” This is not clear from the figure.

20 **We have revised the manuscript, as that we observe dry conditions in the middle troposphere and relatively wetter conditions near the tropopause.**

p7, l. 2: “The ARM 95-GHz W-band ARM ...” one of the two ARMs seem redundant.

**Agree.**

p7, l. 32: "highlighting locations...ARSCL methods." It seems to me that the determination of cloud-top is improved by RWP, and cloud-base by MPL. Is this summary correct?

5

**Yes.**

p8, l. 16: "... Table 2." Please see my first comment. It would be helpful to mention at this point that a variation of Table 2 is plotted in Figures 10 and 11.

10

**Ok.**

p8, l. 18: "Measurable precipitation (> 1 mm) ... light/trace precipitation (< 1 mm)." Is this accumulated precipitation over one day or one hour?

15

**This was in reference to the total daily precipitation. Fixed.**

p8, l. 24: "... below normal ..." A number representing the "normal" accumulated precipitation could be helpful.

20 **Fixed.**

p8, l. 27: "...convective and stratiform ..." Please see my third general comment.

**As above.**

25

p9, l. 30: "inspection of large-scale ... thermodynamics." Totally understandable statement, but isn't it true that the diurnal cycle of high-level clouds is tied to the diurnal cycle of the large-scale dynamics and thermodynamics through deep convection?

30 **Interesting comment. We have attempted to reword.**

p10, l. 13: "profile methods also distinguish columns with convective vertical air motions... as 'convective'." Please see my third general comment. And further details regarding the profiler methods could be informative.

Added.

p10, l. 24: “the difference in the mean rainfall rate are less pronounced, implying dry season convection as stronger (instantaneously), since the convective cell coverage is also reduced during the dry season ...” Recently Schiro 2017  
5 (Thermodynamic Controls on Deep Convection in the Tropics: Observations and Applications to Modeling) examined animated radar data for the GoAmazon campaign period, and reached a similar conclusion.

**Thank you for the reference. Added. We assume you are referring to the dissertation,**

10 **Schiro, K. A.: Thermodynamic Controls on Deep Convection in the Tropics: Observations and Applications to Modeling, Ph.D. thesis, University of California, Los Angeles, Los Angeles, CA, 148 pp., 2017.**

p10, l. 28: “organized systems pass over T3 primarily in the morning hours during  
15 the wet season...” Is this consistent with Figure 8(d)?

**Yes; The secondary peak in deep convective clouds between 23-03LT, is likely associated with propagating convection passing over T3 site.**

20 p10, l. 32: “...with the dry season having less organized cloud contributions...” Will Figure 9 be similar to Figure 8 if both figures are composed for only precipitating days?

**Unlikely. If we just consider the case of ‘deep’ cloud classifications, one might expect significant differences in the diurnal properties of those clouds simply owing to those from the wet season more likely having organized/MCS-type  
25 trailing stratiform components than the more-likely isolated convective dry season storms (having less stratiform components).**

p11, l. 3: “... stratiform...” Please see my third general comment.

30 **Ok.**

p11, l. 6: “... consistent with a response to increased surface heating and an increase in the surface latent heat flux ...” The increments are defined with respect to certain reference values, but it is not clear what these reference values are.

**This is unclear for the authors. Is the reviewer asking for reference values to the increased surface heating / surface latent heat flux in the morning hours as compared to other times of the day? Surface heat flux responds to solar forcing and has a similar diurnal cycle with downwards SW flux. In that sense, we expect both latent and sensible heat flux to increase from sunrise to local solar noon.**

5  
p11, l. 13: "This pattern suggests ... under wet season conditions." If the shielding issue mentioned right after this statement is real, the pattern is also due likely to the suppressed contrast of cirrus cloud, isn't it?

**Our interpretation was that this implies that the contrasts we observe could be even more pronounced – that the wet season pattern could be missing some fraction of these cirrus clouds and the separation between the two seasons (if one was comparing longer term model regime statistic behaviors).**

10  
p12, l. 22: "... sample sizes are potentially too small ..." Please see my first general comment. Including uncertainty/variability is a potential solution.

15  
**As in response to those general comments.**

p12, l. 31: "...precipitating convective clouds..." Please see my third general comment. The definition of precipitating and non-precipitating clouds, i.e., the threshold, is not clear.

20  
**As above.**

p16, l. 15: "...suggest clouds influenced by aerosol tend to have larger concentration of smaller droplets and fewer precipitation sized drops for clouds with similar LWC." With the evidence presented in the manuscript (no information about chemical composition, though seasonal wind direction might implicate), it is unclear that how the wet-vs-dry season contrast for larger-scale environment dynamic/thermodynamic conditions would affect the cloud-microphysical processes (e.g., collision-coalescence, precipitation scavenging, ... I suspect that this question can only be answered by later modeling studies), I would modify this sentence as something like "... is consistent with the hypothesis that clouds influenced by aerosol tend to have larger concentration of smaller droplets and fewer precipitation sized drops for clouds with similar LWC."

30  
**Accepted.**

Figure 2(a), I suppose the hydrometeor frequency is defined with respect to a threshold. Assuming this is true, it would be nice to know the threshold.

5 **We use ARSCL cloud masking as part of this, which depends on the source of the dataset (e.g., WACR, MPL). For RWP, echoes with  $Z \geq -10$  dBZ are considered significant hydrometeor return. Both undergo filtering for significant echo based on other fields (for example, echo classification schemes to remove Bragg echo-dominated regions from the RWP)**

10 Figure 2(c), two additional horizontal lines could help the readers better capture the evolution of CAPE and CIN.

**We have attempted to modify several images as best as could satisfy multiple reviewer comments. This includes adding horizontal lines in Figure 2c for the corresponding mean value of CAPE and CIN to address the reviewer's suggestion.**

15

Figure 5(d), the rain rate is discretized with non-trivial units.

**Ok. Added to figure caption.**

20

Figure 7(b), it is not clear in the caption how a precipitating day is defined by the condition  $> 1$  mm/hr. Does it mean the daily accumulated precipitation  $> 24$  mm, or hourly accumulated precipitation  $> 1$  mm for any hour of the day (also note p12, l. 28)?

25

**Correct; reference to daily precipitation, [mm], not an [mm/hr] threshold. Fixed.**

Figure 7(c), it is not clear that whether the fractions are calculated for all days or for  
30 only precipitating days.

**Relative to the total precipitation that was collected in those intervals; Thus, it would then only be applicable for precipitating days.**

35

Figure 10(a), the frequency of altostratus is 0 from 6 to 16 (assuming my reading of the color bar is accurate). Following the usual definition of conditional average, the frequency should be in the denominator. If this is how conditional SW CRE is defined, how could it be well defined for the same period when frequency is 0?

- 5 **The original figure had some errors in the white color. The altostratus frequency are quite low (< 1%) but not zero. The figure has been updated.**

Figure 12(f), The units of LWP are g/kg, which is different from the conventional definition and Figure 5(d). A typo maybe?

10

**Yes. Image has been corrected.**

## Response to Anonymous Referee #2

### Overview

5 *This manuscript presents a nice overview of unique datasets from the central Amazon, specifically focusing on vertical profile measurements of thermodynamic conditions and cloud boundaries with collocated surface radiative flux observations. It doesn't get into much detail on any one science question, but that is okay for an overview paper, especially since these datasets are not discussed in detail in Martin et al. (2016, 2017) overview papers. The results showing differences between wet and dry seasons are expected from previous studies, and the most interesting new results are the*

10 *estimated cloud radiative effects of different cloud types as a function of season and diurnal cycle showing mean properties over a year that are similar to shortwave and longwave cloud radiative effects at a very rainy site in the Tropical Western Pacific. Another interesting finding is that cumulus clouds tend to be deeper with greater liquid water paths in the wet season than the dry season despite similar liquid water contents in the clouds and larger droplets in the wet season clouds. My primary concern is that the authors don't delve far enough into these interesting findings leaving the paper very*

15 *descriptive with open questions. Being an overview paper of newly available datasets, I don't expect as much scientific investigation as in other types of papers, but I think that there are fairly simple and straightforward ways that the authors could attempt to explore some of the reasons for the aforementioned interesting results, as described further in major comments 5 and 6.*

20 **We thank this reviewer for their comments and suggestions, and we hope we have improved the revised manuscript in ways that respond to any concerns. As this is a combined response to several reviewers, we will attempt to respond directly to comments within this section, but may refer the reviewer to responses (and associated changes) to the other reviewers as well.**

### 25 *Major Comments*

*1. There are a lot of coauthors on this paper, and I can't help but wonder how each coauthor contributed to the paper. Does each coauthor meet ACP's guideline that "only persons who have significantly contributed to the research and paper preparation should be listed as authors"? What did each coauthor contribute?*

30 **We believe that the co-authors have all significantly contributed to the presented research and/or preparation of this manuscript. Overview efforts lend to acknowledging the many contributors required to collect, process, interpret the diverse insights covered by this manuscript.**

2. The CAPE values seem extremely high. For example, they are far higher than those from Manaus in Machado et al. (2004) and in Williams et al. (2002) in Rondonia, Brazil (both papers that you cite). This could be a result of having mid-day soundings, but have you checked to make sure that these are correct? Was any comparison made with the 12 and 00Z Manaus operational soundings? And what is causing the CAPE to rise so dramatically to near 4000 most days? This is an interesting feature. Is this confined to lifted parcels within a thin PBL layer, so that mixing erases much of it and prevents extreme convection from occurring?

For the calculation of convective indices, we follow the methodology outlined in Jensen et al. [2015] and Moncrieff and Miller [1976]; CAPE is calculated as the vertical sum of the parcel buoyancy, calculated as the difference of the parcel virtual potential temperature and the environmental virtual potential temperature divided by the environmental virtual temperature (e.g., see eq. 1 in Jensen et al [2015]).

As the reviewer is likely aware, the calculation of CAPE (and CIN) is very sensitive to the choice of the originating parcel. For the purposes of this manuscript, we used two separate representations of the surface parcel characteristics. We calculate CAPE using the first sounding observations to represent the surface parcel (often referred to as the surface-based CAPE or SBCAPE from Bunkers et al. [2002]), and we also use the level of maximum virtual temperature within the lowest 1 km (this is similar to the “most-unstable” CAPE or MUCAPE from Bunkers et al. [2002]).

Bunkers, M., B. Klimowski, and J. W. Zeitler, 2002: The importance of parcel choice and the measure of vertical wind shear in evaluating the convective environment. Extended Abstracts, 21st Conf. on Severe Local Storms, San Antonio, TX, Amer. Meteor. Soc., P8.2. [Available online at [http://ams.confex.com/ams/SLS\\_WAF\\_NWP/techprogram/paper\\_47319.htm](http://ams.confex.com/ams/SLS_WAF_NWP/techprogram/paper_47319.htm).]

We note that these values often were the same; this approach tends to maximize the value of CAPE for each sounding. Without a quantitative way to determine the level from which a convective parcel originates (impacts of mixing), we choose a single origin for all soundings. Because of this sensitivity to the definition of the surface parcel, comparisons between CAPE values from different studies should be done carefully. We expect that much of this CAPE is never realized due to mixing.

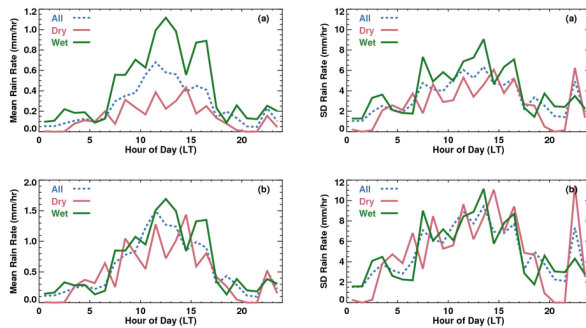
3. Increase the text size on Figure 3. It is currently unreadable. Also, the units in Figure 12a-b are off by 2 orders of magnitude.

Agree. We revised Figure 3 to improve readability. Old Figure 12a-b concentrations were in logarithm scale, the figure has been revised in the revised manuscript.

5 4. The hour to hour noisiness of rain rate in Figure 7 seems to indicate modest sample size, perhaps not surprising for a point location, even if observed for nearly 2 years. Does this impact the robustness of conclusions that require sub-setting of the data (e.g., diurnal cycle, seasonality)? The peak in rainfall at noon is also sooner than is typically observed in most land locations, and it doesn't seem to match up with the peak congestus and deep convection cloud fractions in Figures 6, 8, and 9. Is there a reason for this?

10 As also described in our responses to Reviewer 1/3, we believe the results are consistent with studies that attempt to capture local T3 behaviors as compared to regional-domain behaviors (within a few hundred kilometer distance from the T3 site). For one example of how we have supported this further, this is demonstrated in ShCu comparisons against satellite observations, response to Reviewer 3.

15 For precipitation, we provide Reviewer 1 with the following image that demonstrates the standard deviation of instantaneous rainfall rates. We have also added reference in a new panel in Figure 7 to the total precipitation. There are fewer observations in the overnight hours, but also fewer instances of larger precipitation rates / convection. We agree with the reviewer if their comment is suggesting some variability is to be expected, simply based on having a  
20 single site for a two-year period.



As far as spatial representativeness, we do not agree that the peak we observe at T3 is uncharacteristic. Some confusion (as related to 'deep convective' cloud classifications) is that 'deep convection' cloud categories include the convective cells, convective lines, and the complement of MCS systems (i.e., recent MCS literature refers to as broad

stratiform region, Houze et al. 2015). This includes what we consider as ‘convective’ precipitation, as well as stratiform precipitation components that trail those deeper convective cells.

5 Houze, R. A., K. L. Rasmussen, M. D. Zuluaga, and S. R. Brodzik, 2015: The variable nature of convection in the tropics and subtropics: A legacy of 16 years of the Tropical Rainfall Measuring Mission satellite. *Rev. Geophys.*, 53, 994-1021.

10 Our co-authors in Burleyson et al. 2016 (JAMC) have also shown that the frequency of deep convection around the T3 site begins to increase just before 1200 LT and has a broad peak across the afternoon during the rainy season (their Figs. 8, 10) which we still believe is consistent with our Fig. 8. The SIPAM S-band radar also shows measurable mean precipitation around the T3 site from 0900 – 1800 LT (their Fig. 11), which is consistent with our Fig. 7. Nevertheless, we do agree that some variability in Fig. 7 does arguably reflect some limitations with our sampling (esp. since overnight hours feature fewer instances of rain than afternoon hours, etc.) and some noisiness associated with rain gauge measurements;

15  
20  
25 5. *The similar CRE between Manaus and Manus is interesting, and perhaps expected, especially relative to Darwin and Nauru, which are not typical of many rainy, tropical places because of the dry air aloft that often impacts them. However, breaking down the overall SW and LW CRE at each site by frequency of cloud type and conditional CREs for each cloud type like in Table 2 would be much more interesting. Are some cloud types similar while others are different between sites? How do these similarities and differences impact the overall SW and LW CRE? Are there differences in the diurnal cycle of cloud type frequencies and CREs? Ideally, it would be extremely informative to investigate potential thermodynamic relationships with cloud frequency or CRE at the different sites or to pick a key cloud type like shallow cumulus and relate its CRE with its depth and LWP at each site. I'm not suggesting that I expect you to do all of this, but it seems that it would be fairly straightforward and not very time consuming to investigate a little more, placing this new dataset into better context with other well-observed sites.*

30 The suggestions of this reviewer are interesting and valuable, and a detailed and extended analysis along these lines would be reasonable. However, the authors feel several items may represent a future step for GoAmazon datasets, insomuch that a level of care must be taken to perform the comparison rigorously so that one can understand any differences (rather than rushing this for a revision). As in other comment/responses, initially we found very low correlations between the cloud fractions and thermodynamical quantities of interest, in terms of direct or lag correlations, for various cloud types (e.g., perhaps even more time-consuming when the initial overview flow was not to drill down too heavily on a single cloud type, etc).

Further, digging into the comparisons between sites such as Manus and Nauru, there are interesting similarities and differences in SW CRE by cloud type (and we agree with modifying the manuscript to remind reviewers that the bulk similarities do not necessarily extend to individual cloud type behaviors). The authors note that results in Table 2 (individual cloud types values) can be compared with those from Burleyson et al. (2015) Table 4 (as provided below).

5 For example, while the frequency of shallow clouds (mostly cumulus in these two regimes) is roughly similar, as is their average SW transmissivity, there are differences found in the mean SW and LW CRE for shallow clouds between the two sites.

		Frequency (%)	Frequency as lowest cloud (%)	SW Trn	SW CRE ( $\text{W m}^{-2}$ )	LW CRE ( $\text{W m}^{-2}$ )
Low	Manus	15.9	23.4	0.52	-336.5	27.0
	Nauru	12.2	20.9	0.58	-291.4	26.2
	Darwin	21.1	31.1	0.63	-261.1	23.3
Congestus	Manus	5.8	8.5	0.36	-432.7	30.8
	Nauru	2.1	3.6	0.33	-445.1	30.5
	Darwin	3.7	5.4	0.33	-451.9	34.3
Deep convection	Manus	6.7	9.9	0.19	-539.5	33.1
	Nauru	2.0	3.4	0.17	-576.1	31.0
	Darwin	5.7	8.4	0.16	-560.2	34.9
Altostratus	Manus	11.3	16.6	0.68	-193.5	16.9
	Nauru	5.0	8.6	0.70	-178.3	14.6
	Darwin	7.6	11.2	0.69	-197.6	18.4
Altostratus	Manus	1.2	1.8	0.58	-256.7	20.1
	Nauru	0.4	0.7	0.55	-292.3	19.3
	Darwin	0.8	1.1	0.56	-271.9	22.9
Cirrostratus	Manus	4.1	6.1	0.48	-337.3	18.0
	Nauru	1.4	2.3	0.50	-329.8	14.8
	Darwin	4.3	6.3	0.43	-361.9	20.6
Cirrus	Manus	22.9	33.7	0.78	-129.3	7.4
	Nauru	35.1	60.4	0.83	-100.1	5.3
	Darwin	24.7	36.5	0.82	-114.0	8.4

Now, this could be due to a number of factors: variance in the clear sky downwelling SW or LW flux, the time of day when the shallow clouds are most prevalent, or the frequency of multi-layer clouds (something along the lines of thicker cirrus clouds occurring on top of the shallow clouds – more in Reviewer 3 response). Last to note, in our current study we define shallow cumulus clouds with cloud-top height < 3 km, whereas in Burleyson et al. (2015) the height threshold used was < 4 km. That implies the shallow clouds defined in our study are physically limited to being shallower than those in Burleyson’s study (hence, optically thinner), potentially resulting in smaller SW CRE.

15 Identifying which of these factors are playing a role would help the community better understand the differences in cloud characteristics between the two sites; At present, we do think that this analysis is beyond the scope of what we intended for this overview paper. But, we do agree we should revise and mention that bulk agreement does not necessarily extend to all cloud types, and that these differences are an interesting topic for further study that should be highlighted in the revised manuscript. We have added some discussions of these issues in the revised manuscript.

20

6. Given the datasets available that are highlighted in this paper, it seems like it should be straightforward to investigate the cause of deeper cumulus clouds with greater LWP in the wet season as compared to the dry season, but with similar LWC. Is the cumulus cloud depth related to the CIN, relative humidity just above the boundary layer, both? When cumulus cloud depth is controlled for, do the dry season clouds have a stronger SW CRE caused by greater numbers of smaller droplets? How much of an increase in cloud depth is required to offset the cloud droplet SW CRE? These are questions that could probably be examined without too much effort that are important to understanding how all of these observations connect together through processes.

10 Again, a very interesting science question from the Reviewer, placing a different emphasis on another type of cloud regime within this diverse dataset. While the authors admit our response to this reviewer is possibly nonideal, we initially prioritized (in this set of responses) responding more to the full set of reviewer comments with respect to representativeness or spread of the observations, including additional comparisons against satellite observations. We believe those additions are more important (putting up a fence) as related to adding confidence in these datasets, so as to then be trustworthy as capable/appropriate for activities as outlined above (chasing the livestock).

7. ACP requires a "Data Availability" section on how all research data can be accessed, which goes before the "Acknowledgements" section. Please insert this section.

Added.

Minor Comments

25 1. On page 5, lines 5-7, I have trouble seeing higher CAPE and lower CIN in the transition periods in Figure 2. It looks fairly constant and the CIN appears lowest in the wet season and highest in the dry season, consistent with Figure 3, so can you clarify this sentence or better show it in the figure? It is then stated on page 11, lines 23-24 that wet season conditions favor weaker CAPE and dry season stronger CAPE, but the figure don't seem to show that. There is very little difference in Figure 30 3a, with enough spread that the differences between wet and dry season CAPE is likely not statistically significant.

As also to Reviewer 1, attempted to clarify. We were not clear about our usage of CIN (e.g., magnitudes). We agree that the differences (e.g., reports for slightly higher CAPE in the dry season, etc.) do not appear too pronounced (could be because of the use of radiosonde maximal daily values ); We have added horizontal lines (corresponding to

mean values of CAPE can CIN) in Figure 2 to help show their variability with season. The behavior is arguably more pronounced for Fig. 3, but we have attempted to modify the text to a more conservative stance in line with the ARM observations (as compared to the expectations of previous efforts).

5 2.. On page 5, lines 16-17, it is stated that CIN decreasing during the day with CAPE peaking at mid-day is consistent with development of convection breaking the capping inversion and consuming CAPE, but I don't understand this argument. Isn't the layer of CIN (not necessarily an inversion, by the way) simply reduced through boundary layer mixing induced by daytime heating, while the same daytime heating warms the boundary layer and increases CAPE?

10 **The argument would follow that the CAPE increases and the CIN decreases in the morning portion of the day as the surface is heated and the boundary layer is mixed. As convective parcels reach the level of free convection, CAPE is consumed such that later in the day the CAPE begins to decrease.**

3. Is the moisture advection in Figure 4 the same as moisture convergence? How is it calculated? It is difficult to interpret 3-D advection. How much of the advection in Figure 4 is a result of the vertical component? Can it be stated if vertical mixing is the dominant component?

**The 3-D moisture advection is the same as 3-D moisture convergence, since the difference between moisture advection**

$$-V_h \cdot \nabla_h q - \omega \frac{\partial q}{\partial p} \text{ and moisture convergence } -\nabla_h \cdot (qV_h) - \frac{\partial(\omega q)}{\partial p} \text{ is } -q \left( \nabla_h \cdot V_h + \frac{\partial \omega}{\partial p} \right) \text{ which equals to 0.}$$

20

**We revised the text to add the calculation of total advection:**

*“Fig. 4 plots the diurnal cycle of the large-scale vertical motion (omega), total advection of moisture and relative humidity. The total advection of moisture is the sum of the horizontal and the vertical advections:*

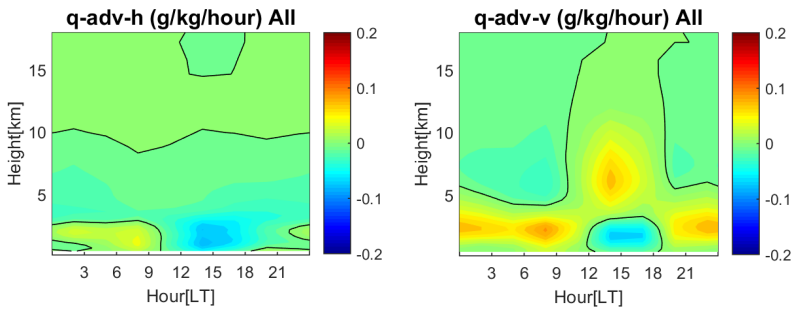
$$q\_adv\_t = -V_h \cdot \nabla_h q - \omega \frac{\partial q}{\partial p}$$

25

*The total advection can be interpreted as 3-D moisture convergence. For the GoAmazon period, the vertical component dominate the total moisture advection (not shown). These large-scale fields were derived ...”*

**The figures below show the horizontal (q-adv-h) and vertical (q-adv-v) moisture advections. The vertical component dominates the total moisture advection.**

30



4. On page 7, it is stated that the RWP is used to reconstruct cloud boundaries up to 13 km, but really, isn't the RWP observing precipitation boundaries due to its sensitivity limitations? And because of these same limitations, doesn't it underestimate cloud top? These seems apparent in Figure 5, for example. If so, I recommend mentioning this limitation.

Agree. We have added some clarification to the text.

10 5. The CRE estimates depend on accurate estimates of the clear sky radiative fluxes. What causes the sharp decrease in clear sky longwave flux at 15Z in Figure 5f that appears coincident with the edge of the deep convective system? Is this accurate? If not, is there a bias in some situations that impacts longwave CRE?

15 The clear-sky LW flux estimates from the RadFlux product (Long and Turner 2008) was derived using actual detected clear-sky data when available, and uses surface measurements of air temperature and vapor pressure in the Brutsaert (1975) formula. As shown in Ohmura (2001) and later confirmed by McFarlane et al. (2013), the first 100 m and first 1 km above surface produce over 70% and over 90% of the clear-sky downwelling LW irradiance, respectively. Since this lowest portion of the atmosphere tends to be well mixed, one can use the surface 2m meteorological measurements to derive a relationship fairly well representative of the gaseous LW emission reaching the surface. Therefore, the drop in downwelling clear-sky LW is associated with the drop in 2m air temperature. But, the clear-sky downwelling LW would also decrease because of the large influence of the near-surface temperature and humidity on the clear-sky LW fluxes.

25 Brutsaert, W., (1975): On a Derivable Formula for Longwave Radiation from Clear Skies, Water Resour. Res., 11(3), 742– 744.

Long, C. N. and D. D. Turner (2008): A Method for Continuous Estimation of Clear-Sky Downwelling Longwave Radiative Flux Developed Using ARM Surface Measurements, *J. Geophys. Res.*, 113, doi:10.1029/2008JD009936.

5 McFarlane, Sally A., Charles N. Long, Julia Flaherty, 2013: A Climatology of Surface Cloud Radiative Effects at the ARM Tropical Western Pacific Sites. *J. Appl. Meteor. Climatol.*, 52, 996-1013. doi: <http://dx.doi.org/10.1175/JAMC-D-12-0189.1> [pnnl-sa-89006]

Ohmura, A. (2001), Physical basis for the temperature-based melt-index method, *J. Appl. Meteorol.*, 40(4), 753– 761.

10

*6. It is mentioned that low level clouds impact the detection of upper level clouds by the micropulse lidar and ceilometer. Is this what caused the discontinuities in cirrus cloud fraction at 6 and 18Z in Figure 6a? If so, can this be stated? And does this mean that cirrus is significantly underestimated at the uppermost levels?*

15

**Underestimation of cirrus is a well-known issue. The drop in daytime cirrus detection by MPL is also likely affected by increase noise due to background solar flux. So, we suggest that it is a combination of low clouds and reduced SNR for the lidar when the sun is up. Below is the relevant text and citations from Burleyson et al. [2015] as related to the SNR issue:**

20

“One characteristic of the active remote sensors that needs to be considered is a reduced sensitivity to optically thin high-level clouds during periods of high solar elevation angles. As demonstrated in Comstock et al. (2002), there is an approximately 30% decrease in high cloud frequency detected by the MPL at Nauru during the 6 h period centered on solar noon when the sun is highest in the sky. This decrease is attributed to poor MPL signal-to-noise ratios when the solar background energy is large, increasing the noise. In addition, the ARM program physically covers the lidar telescope during times when the sun is nearly overhead to avoid damaging the receiver.

25

More recent comparisons between the MPL and Cloud-Aerosol Lidar and Infrared Pathfinder Satellite Observations (CALIPSO; Stephens et al. 2002) confirmed that the fraction of cirrus that is not detected by the MPL during daytime is ~25% for clouds above 10 km (Thorsen et al. 2013). Dupont et al. (2011) showed that almost 50% of situations over the ARM Southern Great Plains (SGP) site show a signal-to-noise ratio too low (smaller than 3) for the MPL to infer cloud properties higher than 7 km using the STRucture of ATmosphere (STRAT; Morille et al. 2007) methodology during summer daylight periods. These limitations suggest that any reduction in the frequency of occurrence of optically thin high-level clouds near solar noon may result from a sampling bias and thus must be interpreted carefully.”

35

7. On page 9, there are several places where the wording doesn't seem accurate:

5 a) On lines 5-6, it is stated that shallow clouds dominate the early morning hours, but to me, it looks like they continue well into the afternoon.

**Adjusted.**

10 b) On line 12, it is stated that congestus and deep convective clouds are prominent from mid-late afternoon, but it looks like they are prominent starting right at noon, and peak cloud fraction looks to be between 12 and 1 PM for congestus and 12 and 2 PM for deep convection rather than at noon, as is stated in the paper.

**Adjusted.**

15 c) On line 21, it is stated that the convection aligns with the mid-upper level vertical motion, but there is a secondary maximum in deep convection overnight when there is descending mid-upper level motion, so these don't seem perfectly aligned to me.

**Adjusted.**

20

d) On line 24, the pre-dawn peak in altocumulus is its primary peak, not its secondary peak.

**Adjusted.**

25 e) Lines 25-27: The wording here is confusing. What does precipitation have to do with congestus cloud fraction peaks? Please clarify.

**By our definitions, the congestus clouds are associated with a nontrivial fraction of the precipitation.**

30 8. Stating that 103 wet season days produce 1600 mm of rainfall and 52 dry season days produce 600 mm of rainfall doesn't necessarily lead to a factor of 2 difference in average rain rate. I can see that differences in Figure 7, but the argument from the number of days and precipitation perspective requires knowledge of how many total wet season and dry season days were sampled.

Agree.

9. The statements on page 10, lines 5-7 and lines 23-25 seem contradictory with one saying that relative convective intensity is not much different between wet and dry seasons, while the other says that dry season convection is stronger. I personally don't see evidence in Figure 7 that dry season rain rates are more intense with conditional rain rates in both seasons that are similar.

The reviewer is correct that nothing presented in Figure 7 (original, or revised) would immediately demonstrate this concept on its own. The key statement in the manuscript was that "...the overall convective cell coverage is also reduced during the dry season (e.g., Giangrande et al. [2016])." This was based on area/temporal convective coverage from that RWP (e.g., same dataset, location, etc.).

10. On page 10, line 28, how are you defining "organized systems"? And similarly, on page 11, line 1, how is "organized cloud" defined?

15

Changed references to mark these as mesoscale convective systems.

11. It's not surprising that clouds and thermodynamics are not strongly correlated when viewed from a stationary vertically pointing perspective, but this shouldn't be confused with them not being correlated over a larger scale from a Lagrangian perspective. When you state that weak correlations are found between cloud behaviors (isn't cloud state a better term here than behavior?) and thermodynamic parameters, what time scale is this correlation being computed on and is it a time lag correlation?

We agree with cloud 'state' and have changed the wording. The initial reference, Collow et al. [2015] and its reference to Kollias et al. [2009] (and associated references within that) as best as we can determine did not factor in the lag correlations within a given day. When we performed our checks on these ideas starting from Collow's reference, we did adjust our calculations to determine the impact for considering different sounding launches (relative to these diurnal variability), but not necessarily ensuring these were always 3h before the time of cloud observations/initiations, 6h before cloud initial observations, etc. Nevertheless, those forms of lag correlations also suggested that nothing generally 'jumped out' as far as significant improvements to those correlations between quantities of interest and sounding parameters. This also relates back to a previous Reviewer 2 general comment, e.g., it is questionable that there are necessarily easy/quick relationships between the thermodynamics and the cloud fractions.

12. On page 12, line 10, I believe you can delete “Compared to SW CRE” to make the sentence read more clearly. This sentence mentions SW CRE being much larger than LW CRE, but SW CRE is 0 at night and the surface energy balance is much different at night than during the day, so a given LW CRE at night, even if small compared to the larger daytime SW CRE, could have just as significant of impacts on variables such as surface temperature, couldn't it?

5  
**Yes. We have deleted those words. LW CRE at night has a much larger effect on surface energy budget compared to daytime.**

13. On page 13, line 2, insert “and” between “(SW)” and “longwave” with a comma after “fluxes”. And on line 29, add an  
10 “s” onto “peak”.

**Ok.**

14. On page 15, line 15, it is stated that sharper CAPE and CIN contrasts during the wet season and transitional periods  
15 enhance the likelihood for deep convection to have organized components. First, how are organized components defined? Second, how is this known? I didn't see any evidence presented that shows this and important components of mesoscale convective system growth such as vertical wind shear were not discussed. Mid-upper level humidity and vertical motion are also potentially important factors aside from CAPE or CIN.

20 **The reviewer is correct. We did not present any evidence in this particular paper that MCS systems are more likely to develop in these transitional regimes. We have modified this line.**

15. Consider rewording “supports local congestus to deeper cloud triggering” on page 15, line 19.

25 **Ok.**

16. On page 16, line 1, consider rewording to “between maritime-like ‘active monsoon’ conditions with widespread clouds and precipitation and continental-like ‘break monsoon’ conditions with less clouds and precipitation, but more intense deep convection”.

30  
**Ok.**

17. On page 16, line 10, insert “cumulus” after “thicker”.

**Ok.**

*18. What is meant by "natural cloud laboratory" on page 16, line 14?*

**5 Removed.**

*19. The last paragraph on page 16 has some confusing wording in spots. For example, the third sentence seems out of place in the paper since the Manaus plume was not discussed at all in this study. Additionally, the last two sentences don't seem worded well. Can you attempt to clarify what is meant in these sentences?*

10

**Adjusted slightly in response also to Reviewer 1.**

### Response to Anonymous Referee #3

#### Overview

This manuscript describe a unique long term set of observations, as well as aircraft IOPs, in the Amazon. These measurements are necessary to help better constrain global climate models and parameterizations of clouds and precipitation for regions, like the Amazon, that have been challenging to simulate. Due to the long term nature of the observations they are able to look at cloud and precipitation over the diurnal and seasonal time scales. Their observations of clouds, are limited from these long term sites due to the nature of their 1D observations. From an aircraft based background or a satellite perspective, these estimates of cloud fraction aren't ideal. The works isn't groundbreaking, but it is a good overview paper of the observations from the project that aren't addressed in the other GoAmazon papers.

**We thank the reviewer for their comments and perspective. We hope our revisions/additions help clarify several concerns.**

15

#### Main Comments

1. How often are multi-layer clouds observed? The authors discuss the fact that if they removed the multi-level cases they wouldn't have enough data for analysis. This is a concern when thinking about sorting data by convective and stratiform. Are these categories meaningful if it's only based on the lower most data? What if there are both convective (low level) clouds and higher level stratiform clouds that are obscured? Does this have an impact on the rain rate? Are the rain rates difference from convective clouds only vs. multi-level clouds?

We note that for precipitating / deep clouds, the presence of multi-layer clouds are not a major concern for our definitions [since deep clouds already occupied the column between low (<3km) and upper (> 8km) atmosphere]. Now, we have examined the frequency of single- and multi-layer clouds (regardless of their cloud types) for the entire GoAmazon dataset, and breakdown this by wet and dry seasons (see the figure below). Over the entire field campaign period, single layer clouds occur ~48% of the time, whereas multi-layer clouds occur ~20% of the time. During the wet seasons, multi-layer clouds occur twice more frequently than during the dry seasons (~28% vs. ~11%).

Now, we suppose the Reviewer's initial comment was in response to our sentence (near the end of the second paragraph in section 4):

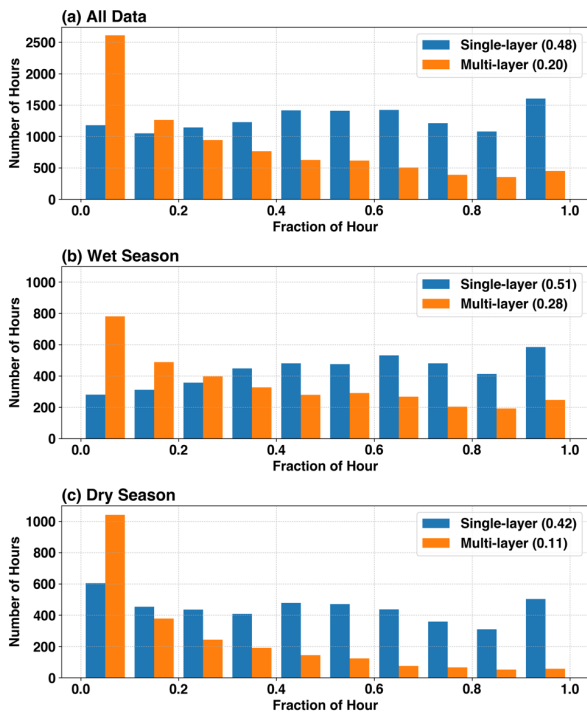
*"However, we also note that it is not possible to separate the radiative impact of multi-layer clouds and sample sizes are potentially too small to only consider single-layer cloud periods."*

What was meant was that it was difficult (sample size) to consider times when we separate by cloud types and then further by hour of the day to estimate their conditional CRE. As seen in the sample size figure in our response to your Comment 2, this includes both single- and multi-layer clouds. Some cloud types (e.g., altostratus, cirrostratus) have rather low sample sizes during certain hours of the day. Further separating single- vs. multi-layer may result in limited samples, not representative of the radiative fluxes associated with those cloud types. We did attempt to examine the potential impact in estimating conditional SW CRE when using single- vs. multi-layer clouds. In section 4.1 second paragraph, we wrote:

10 *"Examination of the averaged conditional SW CRE calculated using only single-layer clouds reveal a relative reduction of ~26% for altocumulus and ~20% for shallow cumulus clouds, and negligible difference in other cloud types."*

While we could choose to use only single-layer clouds, we explained the reason for including multi-layer cloud periods in estimating CRE in the same paragraph:

15 *"Note, the conditional CRE presented in Table 2 includes both single-layer clouds, as well as when additional cloud layers are above the lowest detected cloud layer. This is done deliberately to be consistent with the method used by Burleyson et al. [2015] such that the GoAmazon2014/5 results can be directly compared with their long-term results from the ARM TWP sites."*



2. Estimates of uncertainty are missing and should be addressed. Also, on several figures an idea of the sample size would help put the data into context. It is difficult to evaluate the data when it is unclear how much data is actually included in the figures.

As also in response to Reviewer 1 and 2, we have added references to the degree of uncertainty / spread in some images, tables and the text. Please refer to our detail response to Reviewer #1's first question, which is similar to the uncertainty/variability question this reviewer has asked. In terms of the sample size, we produced a figure below that shows the total number of samples going into calculating the averaged frequency of occurrence of the lowest cloud type. As it can be seen from the figure, all clouds are fairly well sampled (if both single- and multi-layer clouds are

considered). In the dry season, there are a few hour bins for deep convection, altostratus and cirrostratus that have insufficient data sample (< 5 days with those clouds appearing as lowest cloud type at those hours), shown in white colors.

- 5 In some cases, the authors believed the number of events/data were self-explaining, in that it was limited to the same number of days as those in the campaign, etc., with the overwhelming majority of those days featuring clouds and/or precipitation.

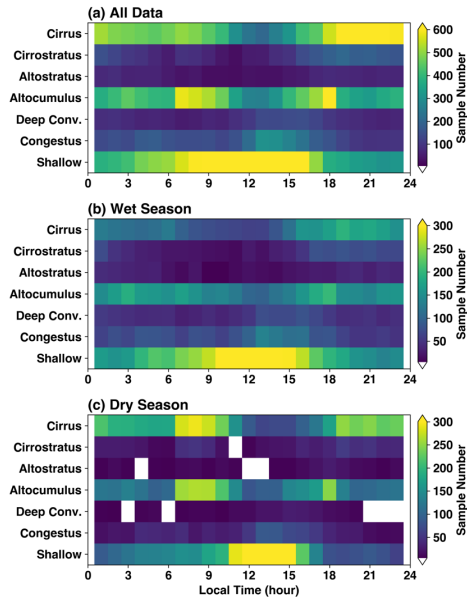


Figure: Number of samples used in calculating average frequency of occurrence of the lowest cloud type for each hour. White bins are hours with less than 5 data samples.

3. I'm confused why they bring in the other locations (Darwin, Nauru and Manus)? These data are not discussed anywhere else in the paper except in section 4 and to add a paragraph in section 5. It seems out of place, it could be part of another paper.

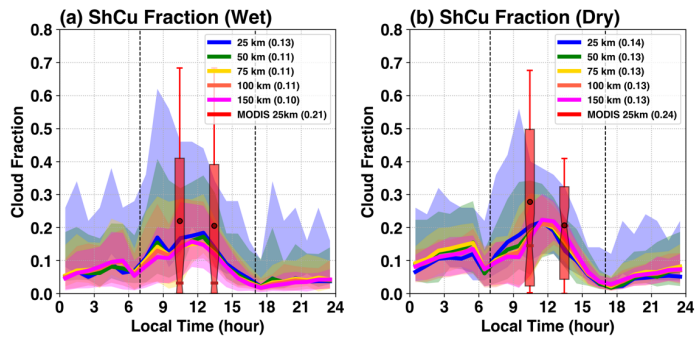
Simply, one motivation was that this dataset that allows new breakdowns of cloud types and contributions to surface radiation budget in the tropics; This is still a very rare observation; Our study provides an opportunity to contrast these results to others at other tropical locations. Or, one of the overarching goals of GoAmazon was to place an additional marker in the tropics for climate studies, particularly for an undersampled region. By comparing/contrasting the CRE effects in the Amazon with those in the Maritime Continent, we may quantify, for example, to what degree a cumulus cloud in one location is similar to a cumulus in another.

4. Have the authors considered using MODIS CF to get an idea how well their CF estimates match satellite observations? They can also use CALIOP to see how their estimates of multi-level cloud classifications compare to the ground measurements. Finally, they can use TRMM or GPCP data to get regional estimates of precipitation. These would put their work into a larger scale context.

As one of the larger additions/responses to this manuscript review, we have performed a comparison between GOES/VISST, MODIS for shallow cumulus (see two figures below). One of these images, and a new discussion, have been added to the revised manuscript as a new subsection 3.3.

GOES VISST/(now SatCORPS) and MODIS datasets were available from Feb-Dec 2014. The GOES product has a 4 km resolution, 30 min update, and the MODIS product has a 1 km resolution and two overpasses. ShCu definition is set as a pixel-level cloud-top height < 3 km (fractions calculated at various spatial coverage domain). Our results show that GOES, MODIS underestimate ShCu compared to T3 (second set of images below), with a larger bias in the wet season than in the dry season. We believe the main reason for this discrepancy is likely the presence of multi-layer clouds obscuring the detection of ShCu from passive satellite sensors (related to a Reviewer comment as above). Spatial mapping of ShCu CF (upper image) suggests that T3 is representative of large area in the central Amazon basin.

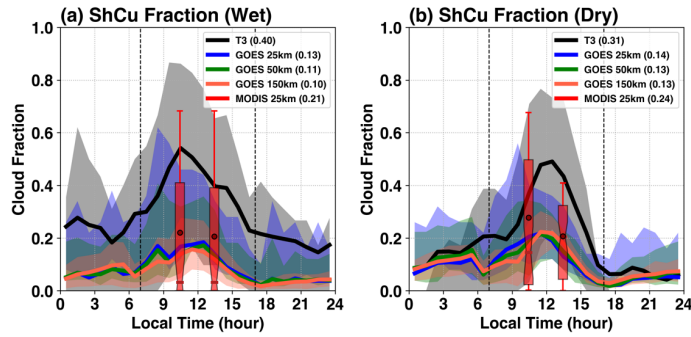
**GOES and MODIS:**



**Key points:**

- Wet Season: Feb 1 – May 1, Dry Season: July 1 – Oct 1
- GOES estimate mean ShCu fractions similar regardless of area.
- MODIS 1 km data provides slightly higher ShCu CF estimates.
- Values in the legend are averaged cloud fraction during daytime (07-17 LT)

**GOES, MODIS, w/ T3 overlaid (New Figure 9):**



**Key Points:**

- GOES underestimate ShCu fraction compared to T3.
- The peak timing of GOES ShCu is roughly comparable to T3.
- MODIS 1 km data provides slightly higher ShCu CF estimates.

15

*Minor Comments*

*There are often generalizations and wording issues that make their points less clear. These issues can be fixed by modifying their text. See specific comments below:*

*Page 2 Line 30 – “cloud study complement to the ...” → “cloud study to complement the...”*

5

**Ok.**

*Page 3 Line 3 – “cloud types and contrasts” what do you mean by “contrasts”, do you mean differences in atmospheric conditions and thermodynamics, seasonal or diurnal changes. This is vague.*

10

**Fixed.**

*Page 3 Line 4-5 – Wording: “This analysis includes additional relationships to campaign aircraft in-cloud observations when available.” → “This analysis includes additional relationships between in-cloud aircraft campaign observations when available.”*

15

**Ok.**

*Page 3 Line 10-11 – What does “possibly maritime-like atmospheric conditions” mean, this is a vague comment and needs clarification.*

20

**Dropped.**

*Page 3 Line 12 – Clarify what you mean by a region of “underlying moisture.” How would you define this, humidity, PW?*

25

**(humidity)**

*Page 3 Line 16 – “work has found a robust relation ...” → “work has found a robust relationship ...”*

30

**Ok.**

*Page 3 Line 19 – Clarify “cloud lifecycle complexity” what complexities are you suggesting are additional versus not-additional, the wording here is unclear.*

Fixed.

Page 3 Line 34 – What are the “environmental forcing data sets?”

5 **Modified as also in response to Reviewer 1.**

Page 4 Line 8 – The pencil-beam/soda-straw description is not necessary.

**Dropped.**

10

Page 4 Line 9-10 – Please elaborate on how CF is described, so 50% cloud cover is recorded when there are cloud present for 30 minutes out of an hour? This seems strange compared to thinking of CF as a fraction of an area if I am interpreting the description correctly.

15 **Yes; For ARM vertically pointing measurements, this is typically done to compare with satellite area cloud fraction estimates (e.g., Xi et al. 2010). It is fairly standard practice within the ASR/ARM DOE and associated climate modeling community.**

20 **Xi, B., X. Dong, P. Minnis, and M. M. Khaiyer, 2010: A 10 year climatology of cloud fraction and vertical distribution derived from both surface and GOES observations over the DOE ARM SPG site. *J. Geophys. Res.*, 115, D12124.**

Page 4 Lines 17-18 – Does this choice, of using the maximum virtual potential temperature, result in a bias towards higher CAPE? Did you try a max, min and mean virtual potential temperatures to see how this changed the results?

25

As also in response to other Reviewers, we attempted two separate commonly used definitions of the surface parcel. We use the max virtual temperature in the lowest kilometer, which is similar to the “most unstable” CAPE (MUCAPE; Bunkers et al. 2002) and we used the lowest sounding observation, or “surface-based” CAPE (SBCAPE; Bunkers et al. 2002). We find that often the value of MUCAPE and SBCAPE are the same (i.e., the max  $T_v$  is at the surface). For the soundings analyzed in this study: SBCAPE and MUCAPE are equal for 56% of the soundings, SBCAPE > MUCAPE for 24% and MUCAPE is larger for 17%. However, we agree we should specify this as ‘MUCAPE’ in the revised manuscript.

30

Page 4 Lines 32 – wording is strange for “on their suitability” I suggest rewording this sentence.

**Ok. Fixed.**

Page 4 Line 32 – Page 5 Line 1 – *What is shown in panel a) of Figure 2. The text here suggests cloud fraction, but the label says “hydrometeor frequency.” Clarify.*

All “cloud fractions” in the paper can also be considered “cloud frequency”, e.g., it is simply a count of cloud occurrences divided by the total number of valid observations within an hour. We have clarified this in the manuscript. The label in Figure 2a has also been changed to “Cloud Frequency” to be consistent with other manuscript figures.

Page 5 Line 7-8 – *Referring to Figure 3, it is not obvious in the CAPE panel that there is a difference between the wet and dry periods. They look the same based on Figure 3a.*

A few reviewers have mentioned this and we have scaled back our language with respect to these differences and their significance.

Page 6 Lines 27-28 – *How are the SCMWF analysis outputs constrained using the surface rainfall? The constraints are not identified in the text. Is it precip or no-precip? A certain amount of precip with a specific threshold? Clarify.*

*Text has been modified to state:*

“These large-scale fields were derived from the ECMWF analysis outputs over the entire field campaign using a constrained variational analysis method of Zhang and Lin [1997]. The upper-level state variables (wind, temperature, moisture) from ECMWF are adjusted to conserve column-integrated mass, moisture and energy. Surface rainfall rate from the SIPAM radar is used as a major constraint. Details of these large-scale fields for the GoAmazon2014/5 deployment can be found in Tang et al. [2016]. This variational analysis was performed...”

Page 7 Lines 31-32 – *(also noted in the figure comments) – where is the red bars located? Are they the thin lines above panel c? If so, a new way to note this should be found, it is not clear or easy to use these bars for the purposes described in the text.*

We increased the width of the color bars above panel (c), and replaced red color (RWP period) with magenta color to enhance readability. Additional figure caption was added to describe these details.

Page 8 Lines 5-6 – Why are there no stratus or stratocumulus categories? The only stratiform clouds are altocumulus and cirrocumulus? Are there just so few of these cloud categories that you are leaving them out?

5 We are assuming the reviewer is asking about “low-level stratocumulus/stratus clouds”. Our cloud type classification algorithm only uses cloud base/top boundary heights to differentiate cloud types. If there are stratus/stratocumulus clouds, they will all be classified as shallow clouds. In reality, stratus/stratocumulus clouds rarely exist at T3 during GoAmazon, because persistent low clouds (i.e., no break in time for many hours) were simply not observed in our dataset. The frequent gaps in time for low clouds are consistent with the nature of shallow cumulus clouds. Therefore,  
10 we denote low clouds as primarily shallow cumulus in this study. For trailing stratiform rain (e.g., behind a convective line in a MCS type system), these regions are included in ‘deep convective’ cloud.

Page 8 Lines 24-25 – You bring up that the 2014-2015 rainy season maybe be different than climatology. Perhaps it would  
15 be beneficial to show a monthly climatology for a long period of time to which you can compare the 2014-2015 rainy season? This way the readers can know how different this particular year is from the climatological average. After reading this comment I was left wondering if these results are just a special case or if they are in fact representative of this region in a general sense.

20 As also in response to other reviewers, this statement was partially influenced by another published GoAmazon2014/5 study that made this particular claim (we acknowledge their efforts as a reference of work ongoing from GoAmazon). We have included the value for a ‘normal’ year. We also highlight Burleyson et al. [2016] who investigated this (and the representativeness of T3 spatially), as also in our previous response to Reviewer 1, as in that response:

25 “The topic was a focus of a related GoAmazon2014/5 effort by some of our coauthors – Burleyson et al. 2016 (JAMC). Their primary finding was that the diurnal cycle of deep convection around the GoAmazon sites is a superposition of locally forced convection and the inland propagation of the previous day’s sea-breeze front. Their climatology showed that deep convection begins around  
30 noon around the sites, and has a broad peak in the mid-afternoon over the T3 site. There is some variability among the various GoAmazon sites that is related to localized circulations generated by the river breezes.

More to the Reviewer’s original comment, the diurnal cycle at the T3 site is generally well  
35 correlated with the region to within a few degrees of the site, but the correlation drops off sharply at distances more than a few hundred kilometers. This is particularly important during the wet

**season. We would encourage the Reviewer (or those reading this response) to download that paper for more information.”**

5 *Page 8 Lines 25-27 – This would be a good place to include a more detailed description of how you calculate the precipitation as a function of convective and stratiform clouds. This is difficult and the method isn’t clearly stated.*

**We have attempted to improve some of these descriptions, also in response to Reviewer 1.**

10 *Page 9 Line 19 – What do you mean by “rare?” How often do these sea breeze intrusions occur? How many times did this happen over the study period? What impact do these intrusions have on the results?*

15 **We removed this term and description (was a poor interpretation by the lead author from a few co-author suggestions). A few of our co-authors (Machado, Burleyson, Schumacher) are currently working on efforts to better communicate these squall line statistics (satellite or radar-based). In some cases, these (and other) authors have already shown that the number of squall lines per year may certainly vary as function of the distance from the coast. Specific to T3, we would not think of it as commonplace for squall lines to reach Manaus (e.g., sampling the same squall line). However, complicating this is that these squall lines, although they may dissipate before reaching Manaus, might argue that some instability or humidity continues to propagate over the site. This added complexity is certainly suggested in looking at the Burleyson et al. [2016] composites.**

20

*Page 10 Line 8 – Please describe how you separate the rainfall rates in to convective and stratiform types. Is this based solely on the cloud classification (as shown in Figure 5 c)?*

25 **We have modified text in these sections. These breakdowns are separate from the cloud classifications, in that ‘deep’ convective clouds will potentially contain ‘convective’ and ‘stratiform’ rainfall contributions. For example, the figure below (Fig. 3 in Giangrande et al. 2016) shows an MCS event from the RWP dataset. “Stratiform precipitation” is defined between ~13:20 UTC to ~17:10 UTC, where a clear bright-band signature is observed; “convective precipitation” is defined between ~11:20 UTC to ~13:20 UTC. But in the cloud type classification, both convective and stratiform precipitation are categorized as “deep convective clouds” as their echo-top heights both exceed 8 km and thickness > 5 km.**

30

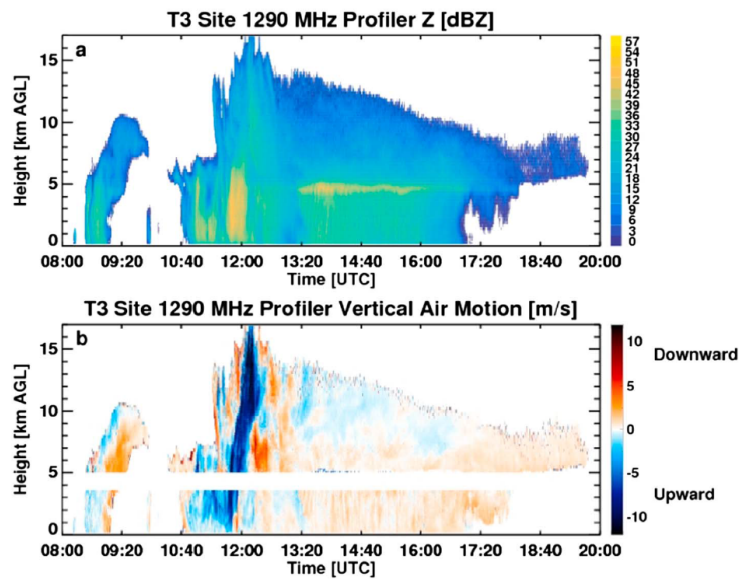


**Figure 3.** Example (a) reflectivity factor Z measurements and (b) vertical velocity retrievals from the 20 March 2014 event during GoAmazon2014/5.

Page 11 Line 3 – “stratiform precipitation (identified as “Deep Convection”...” this is confusing. Do you mean stratiform as  
 5 in cirrostratus? Usually when I see the term stratiform I think of stratus or stratocumulus. Clarify this section.

We have modified some text, but in this context, it would refer most commonly to the trailing precipitation shield  
 behind organized/MCS convective systems – e.g., those regions having pronounced bright band / radar signatures  
 from aggregation/melting.

10 Page 12 Line 14 – The “green ocean” comment again, it’s not really fully discussed in the beginning section (Page 3 Line  
 10) where it is first mentioned so it’s strange to mention it again.

**We have better attempted to reference to the origins of the term in the upper parts of the manuscript. The concept is one of a so-called hybrid environment for clouds that promotes both continental and tropical type characteristics.**

Page 12 Line 28 – “better” this is not a descriptive term. What makes it better? Be more specific.

5

**Ok.**

*Table Comments*

10 *Table 1-3 – The format of these tables is difficult to read in the current format. I’m assuming that they will be formatted differently when published.*

**We modified the table formats to make them fit in a single page for easier reading for the reviewers. The final format of the table is up to the journal.**

15

*Table 3 – Why are the authors including these other locations that are very far from the Amazon. When reading the text, there doesn’t seem to be a solid justification for this other than to make a quick comparison.*

20 **Observations of this sort are rare. There are few references for tropical behaviors. This also ties back into previous ‘green ocean’ claims by other authors.**

*Figure Comments*

25 *Figure 2 – Continue the IOP dashed lines all the way to the top of the figure through panels a, b, and c. Perhaps make solid lines to section off the wet and dry periods as well. This would be helpful for knowing where the cut offs are. I drew them on myself to make it easier for me to see when they started and ended. What is “hydrometeor frequency” shown in panel a). In the test it suggests CF (Page 4-5 Lines 32 -33 “The more pronounced shifts during the wet season include increased CF in the mid0to- upper troposphere (between 3-10 km, Fig 2a). So is it CF or something else that is being shown as frequency. Please clarify.*

30

**CF and cloud frequency are interchangeable for this study and this has now been noted in the revised manuscript. We extended the IOP dash lines across all panels as the reviewer suggested, along with some additional modification to the figure suggested by other reviewers to improve readability.**

Figure 3 – Axes labels are small and hard to read. What is going on with the 19 am data for CIN. Why are they essentially a point?

5 For the 14 UTC sounding time the vast majority of soundings have a CIN value of zero (38 of 56 for the wet season and 34 of 39 in the dry season). When CIN is not equal to zero, the values are generally very small. Figure has also been modified for text sizing.

Figure 4 – Hard to read the panel labels for (g), (h), and (i). Perhaps move them outside and next to the left side of the figures for all the panels.

Figure has been modified.

15 Figure 5 – It is difficult to read the label or panel c), it is obscured by the cirrus clouds. The green and red line above panel c), is that the red bars referred to on Page 7 Lines 31-32. If so, these are near impossible to see clearly.

We added a white background to the label in panel (c). We also increased the width of the color bars above panel (c), and replaced red color (RWP period) with magenta color to enhance readability. Additional figure caption was added to describe these details.

Figure 6 – The white contours (starting at 10%) are difficult to see, perhaps increase the line thickness.

We increased the thickness of the white contour lines for Figure 6 and new Figure 8 (combining previous Figure 8, 9 - as suggested by the reviewer).

Figure 7 – For a) How many days are included (are there equal number of days in all the time bins?) b) same as a), how much data is included? c) Define the fractional accumulation more clearly (convective/stratiform). Does the number of samples change for each time bin? Are some time bins 100 samples (80 wet 20 dry) while others are 10 samples (8 wet 2 dry). It would be nice to know how much data is going into these curves.

We have modified this plot to include a total accumulation plot. When attempting to respond to this, we believed this to be more useful than a plot showing # of instantaneous rainfall rate samples (e.g., counts of nonzero rainfall rates, etc.).

Figure 8 & Figure 9 – Perhaps these two can be merged so you can easily compare the difference between the wet and dry seasons. A difference panel, or just showing the difference between wet and dry would be a good way to show where the differences are most pronounced. As with Figure 6, the white contours (starting at 10%) are difficult to see, perhaps  
5 increase the line thickness.

**We thank the reviewer for the good suggestion. Figures 8 and 9 were combined into a single new Figure 8. We kept the order of the cloud types the same with Figure 6, but put wet and dry seasons next to each other to assist in comparison.**

10

# Cloud Characteristics, Thermodynamic Controls and Radiative Impacts During the Observations and Modeling of the Green Ocean Amazon (GoAmazon2014/5) Experiment

5 Scott E. Giangrande<sup>1</sup>, Zhe Feng<sup>2</sup>, Michael P. Jensen<sup>1</sup>, Jennifer M. Comstock<sup>2</sup>, Karen L. Johnson<sup>1</sup>, Tami Toto<sup>1</sup>, Meng Wang<sup>1</sup>, Casey Burleyson<sup>2</sup>, Nitin Bharadwaj<sup>2</sup>, Fan Mei<sup>2</sup>, Luiz A. T. Machado<sup>3</sup>, Antonio O. Manzi<sup>4</sup>, Shaocheng Xie<sup>5</sup>, Shuaiqi Tang<sup>5</sup>, Maria Assuncao F. Silva Dias<sup>6</sup>, Rodrigo A F de Souza<sup>7</sup>, Courtney Schumacher<sup>8</sup> and Scot T. Martin<sup>9</sup>

<sup>1</sup>Environmental and Climate Sciences Department, Brookhaven National Laboratory, Upton, NY, USA

<sup>2</sup>Pacific Northwest National Laboratory, Richland, WA

10 <sup>3</sup>National Institute for Space Research, São José dos Campos, Brazil

<sup>4</sup>National Institute of Amazonian Research, Manaus, Amazonas, Brazil

<sup>5</sup>Lawrence Livermore National Laboratory, Livermore, CA, USA

<sup>6</sup>University of São Paulo, São Paulo, Brazil

<sup>7</sup>State University of Amazonas (UEA), Manaus, Brazil

15 <sup>8</sup>Texas A&M University, College Station, Texas, USA

<sup>9</sup>Harvard University, Cambridge, Massachusetts, USA

*Correspondence to:* Scott E. Giangrande (sgrande@bnl.gov)

20 **Abstract.** Routine cloud, precipitation and thermodynamic observations collected by the ARM Mobile Facility (AMF) and Aerial Facility (AAF) during the two-year DOE ARM Observations and Modeling of the Green Ocean Amazon (GoAmazon2014/5) campaign are summarized. These observations quantify the diurnal to large-scale thermodynamic regime controls on the clouds and precipitation over the undersampled, climatically important, Amazon basin region. The extended ground deployment of cloud-profiling instrumentation enabled a unique look at multiple cloud regimes, at high  
25 temporal and vertical resolution. This longer-term ground deployment coupled with two short-term aircraft intensive observing periods allowed new opportunities to better characterize cloud and thermodynamic observational constraints as well as cloud radiative impacts for modeling efforts within typical Amazon ‘wet’ and ‘dry’ seasons.

Deleted: controls

## 30 1 Introduction

The simulation of clouds and the representation of cloud processes and associated feedbacks in Global Climate Models (GCMs) remains the largest source of uncertainty in predictions of climate change [Klein and Del Genio 2006; Del Genio 2012]. Collecting routine cloud observations to serve as constraints for the improvement of cloud parameterizations  
35 represents an ongoing challenge [e.g., Mather and Voyles 2013], but one necessary to overcome deficiencies in GCM cloud characterizations. Compounding this challenge, cloud-climate feedbacks operate over extended spatiotemporal scales, while cloud behaviors vary significantly according to the regionally varying forcing conditions [e.g., Rossow et al. 2005]. There is

additional demand to observe and model cloud processes and feedbacks across many undersampled regions, including climatically important tropical locations where it is often difficult to deploy ground equipment.

As introduced by Martin et al. [2016a; 2017], the Observations and Modeling of the Green Ocean Amazon (GoAmazon2014/5) Experiment was motivated by demands to gain a better understanding of aerosol, cloud and precipitation interactions on climate and the global circulation. The Amazon forest is the largest tropical rainforest on the planet, featuring 5 prolific and diverse cloud conditions that span ‘wet’ and ‘dry’ precipitation regimes. These regimes, and associated variations in cloud types, coverage and intensity from sub-daily to seasonal scales, are interconnected to large-scale shifts in the thermodynamic forcing and coupled local cloud-scale feedbacks [e.g., Fu et al. 1999; Machado et al. 2004; Li and Fu 2004; Fu and Li 2004; Misra 2008]. The inability of GCMs to adequately represent clouds over such a complex and 10 expansive tropical area sets apart GoAmazon2014/5 as an important asset for the improvement of GCM cloud parameterizations and simulations of possible climate change [e.g., Williams et al. 2002; Richter and Xie 2008; Nobre et al. 2009; Yin et al. 2013].

One key component for cloud lifecycle and process studies during GoAmazon2014/5 was the two-year deployment of the Atmospheric Radiation Measurement [ARM; Stokes and Schwartz 1994; Ackerman and Stokes 2003] Mobile Facility 15 [AMF; Miller et al. 2016] 70 km to the west of Manaus in central Amazonia, Brazil [3°12'46.70" S, 60°35'53.0" W]. This location was chosen to sample the extremes of the local pristine atmosphere, as well as the effects of the Manaus, Brazil pollution plume. The AMF was equipped to capture a continuous record of column cloud and precipitation characteristics from multi-sensor profiling instrumentation, while routine surface meteorology and flux measurements along with balloon-borne radiosonde measurements provided information on the local thermodynamic state [e.g., Kollias et al. 2009; Xie et al. 20 2015; Tang et al. 2016]. Deploying such an extended, comprehensive cloud instrumentation suite of this sort is unique to Amazon basin studies and rare within global climate-cloud-interaction studies overall, particularly in the tropics. From this dataset, longer-term composites and statistical perspectives on diurnal to seasonal cloud variability (e.g., cloud development, morphological transitions, precipitation occurrence, and radiative properties) are possible.

The long-term, ground-based measurements during GoAmazon2014/5 were complemented with aircraft-based 25 measurements using the DOE ARM Gulfstream-1 (G-1) aircraft (ARM Areal Facility (AAF), e.g., Schmid et al. [2016]). The G-1 was equipped with instruments for measuring clouds, aerosol, chemistry and atmospheric state [e.g., Martin et al. 2017], which provide additional aerosol and cloud microphysical information that is not readily measured at the surface. These data help with the interpretation of ground-based measurements, while the ground measurements assist when determining the representativeness of these aircraft data.

30 This GoAmazon2014/5 cloud overview serves as a focused cloud study to complement the campaign overview effort found in Martin et al. [2017] and is outlined as follows. Section 2 introduces the AMF instrumentation and methods used for cloud

Deleted: to

classification and composite cloud properties. A two-year summary of the environmental conditions and cloud observations in terms of fractional cloud coverages are presented in Section 3. These observations are segregated according to cloud types associated with large-scale Amazon wet and dry precipitation regimes. Section 4 details the observations for individual cloud types and their relative impact on surface energy and fluxes. This analysis includes additional relationships between campaign aircraft in-cloud observations when available. A brief discussion and summary of the initial cloud insights from the GoAmazon2014/5 deployment are found in Section 5.

**Deleted:** and contrasts

**Deleted:** to

## 2. ARM Mobile Facility Cloud Observations

The AMF was deployed in Manacapuru, to the west of Manaus in central Amazonia, Brazil (Fig. 1, herein “T3” site; Martin et al. [2017]). Cloud observations were obtained near-continuously over a period from February 2014 through December 2015. The Amazon region surrounding T3 is often identified as the ‘green ocean’, in reference to its unique atmospheric conditions that exhibit tropical and continental cloud characteristics [e.g., Williams et al. 2002]. The T3 site is situated nearby the intersection of the large Amazon (Rio Solimões) and Rio Negro rivers (Fig. 1), a region of abundant moisture (humidity). As a consequence, T3 and the Manaus region may experience increased cloudiness and unique precipitation cycles as compared to the conditions over the larger Amazon basin [e.g., Oliveira and Fitzjarrald [1993], Silva Dias et al. [2004], Romatschke and Houze [2010], Dos Santos et al. [2014]]. Collow and Miller [2016] recently showed that the presence of the nearby rivers contributed to spatial variability in the regional radiation budgets around the AMF site. Recent GoAmazon2014/5 work has found a robust relationship between column-integrated water vapor and precipitation over the Amazon [Schiro et al. 2016]. Seasonal thermodynamical shifts, as well as additional large-scale sea-breeze front type intrusions into the basin (e.g., Cohen et al. [1995], Alcântara et al. [2011]), promote additional cloud lifecycle and diurnal cycle of precipitation variability (e.g., Burleyson et al. [2016], Saraiva et al. [2016]). Readers are also directed to complementary GoAmazon2014/5 studies on the large-scale environmental controls on clouds, cloud transitions and precipitation found in Ghatge and Kollias [2016], Tang et al. [2016], Collow et al. [2016] and Zhuang et al. [2017]. Our analysis focuses on the T3 site that captured a wide range of shallow to deep cloud conditions, sampled and categorized using multi-sensor AMF methods detailed in this section. Larger-scale forcing datasets (including advective tendencies and vertical velocities) over this region were also supported by domain precipitation estimates available from the System for the Protection of Amazonia (SIPAM) S-band radar operated at the Ponta Pelada airport (“T1”, in Fig. 1).

**Deleted:** , possibly maritime-like

**Deleted:** underlying

**Deleted:** complexity and

**Deleted:** Continuous

**Formatted:** Font:Not Bold, Not Italic

**Deleted:** environmental forcing datasets

We characterize cloud and precipitation properties according to seasonal and diurnal cycles that separate the observed cloud characteristics between relatively ‘wet’ (herein, December through April) and ‘dry’ (herein, June through September) season behaviors. While transitional months (May, October, and November) are not an emphasis of this study, these months contain several intense (e.g., updraft strength and rainfall rates) deep convective events in the GoAmazon2014/5 record. Thermodynamic profiling (radiosonde) and environmental forcing datasets as sampled over the T3 location are summarized

in Section 2.1. To better anchor cloud properties within these wet and dry regimes, aircraft flight operations during GoAmazon2014/5 prioritized two Intensive Operating Periods (IOPs: 1 February - 31 March, 2014, and 15 August - 15 October, 2014) as introduced in Section 2.2.

5 Traditionally, Cloud Fraction (CF) observations are of high interest within the GCM community and for high-resolution climate model evaluation [e.g., Bedacht et al. 2007; Wilkinson et al. 2008]. Cloud breakdowns within our study focus on the diurnal to seasonal controls on these CF estimates. This is accomplished by segregating CF properties according to the results of a cloud-type classification algorithm. The multi-sensor approach and cloud classification methods are described in Sections 2.3 and 2.4. Note, the interpretation of CF estimates and 1D column CF estimate representativeness is often  
10 nontrivial [e.g., Wu et al. 2014]. This study defines CF as the fraction of observations (height-resolved, or over the entire column) within an hour for which the combined profiling sensors identify clouds overhead. In this study, cloud fraction and cloud frequency are used interchangeably.

Deleted: (or, pencil-beam/soda-straw)

### 2.1. Radiosonde, Surface Meteorology and Large-scale Forcing Dataset Overview

During the campaign, radiosondes were launched over T3 at regular 6-h intervals (1:30, 7:30, 13:30 and 19:30 LT, Vaisala  
15 RS-92 radiosondes; ARM [1993]). For the IOPs, one additional radiosonde was launched at 10:30 LT to enhance diurnal coverage. Basic thermodynamic processing was performed following Jensen et al. [2015] to estimate convective forcing parameters such as the Lifting Condensation Level (LCL), Mixed-Layer Height (MLH), Convective Available Potential Energy (CAPE), and Convective Inhibition (CIN). For each of these parameters, surface parcels are defined by the level of the maximum virtual temperature in the lowest kilometer. This represents the most buoyant parcel in the boundary layer and  
20 maximizes the calculated CAPE (thus, our reported values are comparable to 'most unstable' CAPE or MUCAPE). The MLH is calculated using the definition of Liu and Lang [2010] that determines the MLH from a combination of the gradient of potential temperature and the vertical wind shear using criteria based on the stability of the boundary layer and the presence of a low-level jet. Surface radiative flux estimates for this study follow the radiative flux analysis methods of Long and Ackerman [2000] and Long and Turner [2008]. The clear-sky radiative flux estimates are produced by employing an  
25 empirical function fitting approach during observed clear-sky periods. The fitted coefficients from these clear-sky intervals are used to interpolate over cloudy periods, providing a continuous estimate of clear-sky irradiances and quality-controlled cloudy-sky fluxes. Detailed analyses of cloud radiative effects are located in Section 4.

Figure 2 presents the cumulative time-series for the two-year GoAmazon2014/15 dataset in terms of average daily profile  
30 values for basic cloud, precipitation, thermodynamical and dynamical observations from multi-sensor ground instruments at the T3 site. These efforts complement previous manuscripts on seasonal variability for cloud conditions over the larger Amazon basin [e.g., Machado et al. 2004]. We observe clear shifts in several quantities associated with the Amazon wet and

dry seasons. Our ranges for wet and dry season months, as well as the IOP periods, are shown in Fig. 2 as a reference to the appropriateness for those windows compared to the larger-scale conditions. The more pronounced shifts during the wet season include increased CF in the mid-to-upper troposphere (between 3-10 km, Fig. 2a), higher precipitation rates (over these daily integrations) and precipitable water (PW, Fig. 2b), as well as the buildup of relative humidity (RH) profiles through the mid-levels (Fig. 2d). Previous studies suggest that CAPE, CIN and zonal/meridional winds (Figs. 2c, e and f) from radiosondes may also illustrate large-scale thermodynamical changes and moisture transport associated with wet, dry and transitional periods [e.g., Li and Fu 2004; Fu and Li 2004]. Radiosonde daily maximum values indicate only small seasonal changes in CAPE and CIN, although we observe that the transitional periods between the dry and wet seasons promote maximum relative CAPE trends coupled with relatively lower CIN and heightened moisture. These are the primary ingredients that promote more frequent and strong convection, provided convection can be triggered [e.g., Machado et al. 2004]. Although areal coverage of deeper convection is generally the largest during the wet season, recent profiler-based studies suggest the strongest storms (in terms of upward vertical air motion) were often observed towards the end of the dry season and into the transitional period (e.g., Giangrande et al. [2016], Nunes et al. [2016]).

**Deleted:** have been indicated  
**Deleted:** for  
**Deleted:** on their suitability

The diurnal variation of atmospheric state is illustrated by Fig. 3 and shows the evolutions for the mean and standard deviation of (a) CAPE, (b) CIN, (c) LCL and (d) MLH separated into dry (red bars) and wet (blue bars) components [e.g., Betts et al. 2002]. CAPE increases after sunrise, reaching a maximum near midday, whereas CIN is maximum (largest negative value) overnight and decreases during the day. These behaviors are consistent with development of convection breaking the capping inversion and consuming CAPE. Both CAPE and CIN show a stronger diurnal cycle during the dry season compared to the wet season. The mean LCL increases by approximately 600-800 m from sunrise to the afternoon with larger magnitudes and range during the dry season. The mean MLH also increases by approximately 1 km from sunrise through the afternoon during the wet season, while during the dry season the increase is about 1.5 km. This increase in MLH is consistent with daytime solar heating. Separating the diurnal cycle into dry (red bars) and wet (blue bars) season components indicates slightly stronger diurnal cycle signatures in CAPE, increased CIN (e.g., larger negative values) and higher MLH for the dry season (similar to measurements obtained in the SW Amazon by Fisch et al. [2004]), with a suppressed diurnal cycle in LCL height.

**Deleted:** Although r  
**Deleted:** we  
**Deleted:** typically

To better inform the observed cloud system variations over the ARM T3 site from the large-scale environmental condition perspective, Fig. 4 plots the diurnal cycle of the large-scale vertical motion (omega), total advection of moisture and relative humidity. The total advection of moisture is the sum of the horizontal and the vertical advection.

**Formatted:** Font:(Default) +Theme Headings (Times New Roman)  
**Formatted:** Font:(Default) +Theme Headings (Times New Roman), Not Bold  
**Formatted:** Font:(Default) +Theme Headings (Times New Roman), Not Bold  
**Formatted:** Font:(Default) +Theme Headings (Times New Roman), Not Bold  
**Field Code Changed**  
**Deleted:** Fig. 4 plots the diurnal cycle of the large-scale vertical motion (omega), total advection (sum of horizontal and vertical) of moisture and relative humidity  
**Formatted:** Font:(Default) +Theme Headings (Times New Roman)

$$q_{adv_t} = -V_h \cdot \nabla_h q - \omega \frac{\partial q}{\partial p} \quad (1)$$

The total advection can be interpreted as 3-D moisture convergence. For the GoAmazon2014/5 period, the vertical component dominated the total moisture advection (not shown). These large-scale fields are derived from the ECMWF analysis outputs over the entire field campaign using a constrained variational analysis method of Zhang and Lin [1997]. The upper-level state variables (wind, temperature, moisture) from ECMWF are adjusted to conserve column-integrated mass, moisture and energy. Surface rainfall rate from the SIPAM radar is used as a major constraint. Additional details on these large-scale fields for the GoAmazon2014/5 deployment can be found in Tang et al. [2016]. This variational analysis is performed at 3 hourly intervals at 25 hPa vertical resolution over a domain of about 110 km in radius, with the center located at the T1 site (Fig. 1).

The omega field shows strong upward air motion in the middle and upper troposphere during the mid to late afternoon (Fig. 4a). The evening and early morning hours exhibit upward air motion confined below 3-4 km due to lower-level convergence and middle-level divergence (not shown), likely corresponding to the congestus clouds. Above that level, downward air motion is dominant. This downward motion is most pronounced between 0600 and 0900 LT. After sunrise, we observe low-level weak ascending motions and positive advection of moisture (Fig. 4d). Between 4-8 km in the RH field, we observe dry middle tropospheric conditions and relatively wetter conditions near the tropopause (Fig. 4g). Similar structures in all fields are found across wet and dry season breakdowns, however, middle and upper level descending motions during the evening and early morning hours are much stronger during the dry season, suppressing convection during those hours. In addition, the ascending motion between noon and late afternoon is much weaker in the dry season compared to the wet season. The dry season also exhibits reduced low-level positive moisture advection and a much dryer lower and middle atmosphere.

## 2.2. The AAF Aircraft Dataset

The DOE AAF G-1 aircraft participated in two IOPs that coincided with the AMF deployment. Airborne measurements were conducted during 22 Feb. - 23 Mar. 2014 and 6 Sept. - 4 Oct. 2014 representative of the wet and dry season, respectively. The G-1 flight patterns were designed to sample shallow and growing cumulus convective clouds that formed downwind from Manaus to examine the evolution of urban pollution and its effect on cloud and precipitation properties [Martin et al. 2017]. Typical flights consisted of a series of level legs flown just below cloud base, just above cloud base, and higher in growing cumulus clouds, including legs over the T3 ground site. In total, sixteen and nineteen flights in warm cumulus clouds were included in the wet and dry season, respectively.

The G-1 payload was designed to measure the full spectrum of aerosol size from 0.015  $\mu\text{m}$  to 3  $\mu\text{m}$  and cloud particle sizes from 2  $\mu\text{m}$  to 1.92 cm. For this study, three cloud particle distribution probes are combined to create the full drop-size distribution (DSD) depictions presented in Section 4. The Droplet Measurements Technologies Cloud Droplet Probe (CDP; 2-50  $\mu\text{m}$ ) is combined with the Spec Inc. 2-Dimensional Stereo probe (2-DS; 10  $\mu\text{m}$  - 3 mm) between 20 and 50  $\mu\text{m}$  by

<b>Formatted:</b> Font:Not Bold, Not Italic
<b>Formatted:</b> Font:Not Bold
<b>Deleted:</b> These large-scale fields were derived from the ECMWF analysis outputs over the entire field campaign constrained using the surface rainfall rate from the SIPAM radar following the variational analysis method of Zhang and Lin [1997], updated with using Numerical Weather Prediction analysis in Xie et al. [2004] and again as in Tang et al. [2016] for the GoAmazon2014/5 deployment.
<b>Formatted:</b> Font:(Default) +Theme Headings (Times New Roman)
<b>Deleted:</b> wa
<b>Formatted:</b> Font:(Default) +Theme Headings (Times New Roman)
<b>Formatted:</b> Font:(Default) +Theme Headings (Times New Roman)
<b>Formatted:</b> Font:(Default) +Theme Headings (Times New Roman)
<b>Deleted:</b> ,
<b>Formatted:</b> Font:(Default) +Theme Headings (Times New Roman), 10 pt
<b>Formatted:</b> Font:(Default) +Theme Headings (Times New Roman)
<b>Formatted:</b> Font:(Default) +Theme Headings (Times New Roman), Not Bold, Not Italic
<b>Deleted:</b> whereas
<b>Formatted:</b> Font:(Default) +Theme Headings (Times New Roman)
<b>Deleted:</b> a
<b>Formatted:</b> Font:(Default) +Theme Headings (Times New Roman), 10 pt, Not Bold
<b>Deleted:</b> in the RH field
<b>Formatted:</b> Font:(Default) +Theme Headings (Times New Roman)

averaging the overlapping bins. The Spec Inc. High-Volume Precipitation Spectrometer (HVPS; 150  $\mu\text{m}$  – 1.92 cm) is used for droplets larger than 500  $\mu\text{m}$ . Cloud droplet distributions are combined by averaging the DSD for each instrument separately over these flight periods. This was done for in-cloud conditions only. DSDs from the CDP are used for drops smaller than 20  $\mu\text{m}$ . The DSDs from the CDP and 2-DS are averaged between 20 and 50  $\mu\text{m}$ , 2-DS DSDs are used between 50 and 500  $\mu\text{m}$ , and HVPS DSDs are used for drops larger than 500  $\mu\text{m}$ . The 2-DS probe occasionally contained artifacts known as ‘stuck bits’, i.e., when a photodiode becomes continuously occulted due to optical contamination or electronic noise [Lawson et al. 2006]. Each flight was visually inspected for artifacts, which were manually removed from the combined DSDs. Cloud condensation nuclei (CCN) were measured with a dual-column system manufactured by DMT (operated with a constant pressure inlet at 600 mbar), and Liquid Water Content (LWC) was measured using a multi-wire element probe (Science Engineering Associates (SEA) Water Content Meter WCM-2000) with wire sizes the same as King and Johnson-Williams probes.

### 2.3. Radar Dataset and Multisensor Merging

The 95-GHz W-band ARM Cloud Radar (WACR) [e.g., ARM 2005; Giangrande et al. 2012] is the primary profiling instrument to characterize the cloud conditions during GoAmazon2014/5. Cloud masking and designation products are performed using the multi-sensor WACR preprocessing approach following Active Remote Sensing of Clouds methodologies [ARSCL; Clothiaux et al. 2000; Kollias et al. 2005, 2009], and additional quality control refinements following Kollias et al. [2014]. These retrievals merge observations from the WACR and a collocated laser ceilometer, micropulse lidar (MPL), and microwave radiometer (MWR) to better identify cloud boundaries in the vertical at high temporal (~10s) and vertical (~24m) resolution.

There are several limitations when designating cloud boundaries and hourly CF observations from vertically pointing cloud radars beyond the capabilities of single radar platforms or ARSCL methods [e.g., Lamer and Kollias 2015; Oue et al. 2016]. Primary among these is that the WACR experiences attenuation in rain that manifests as erroneously low or missing cloud top boundaries [e.g., Feng et al. 2009, 2014]. To lessen these impacts within this Amazonian deployment that favors frequent precipitating cumulus, a collocated and well-calibrated 1290-MHz UHF radar wind profiler (RWP; 8-degree beamwidth, 200-m gate spacing, 6-s temporal resolution) was co-gridded to improve cloud coverage through deeper precipitating clouds [e.g., ARM 2009; Giangrande et al. 2013, 2016]. For this study, a modification to the ARSCL cloud boundary designation is produced by merging RWP profiles (operating in ‘precipitation’ modes, as also described in Tridon et al. [2013]) during precipitation intervals following similar ARSCL-type cloud profile processing [Feng et al. 2014]. The substitution is accomplished using collocated surface rain gauge datasets to help define appropriate “precipitation periods”. These are defined as continuous time periods when the surface rain rate from the gauge exceeds 1 mm h<sup>-1</sup>. During these intervals, if

Deleted: ARM

more than 10% of the derived WACR first echo-top heights associated with these precipitating clouds is found to be 500 m or more below the echo-top height as recorded by the RWP, a WACR attenuation flag is assigned and the RWP profiles and boundaries are inserted.

5 Figure 5 illustrates an example of the composite cloud designation for the 1 April 2014 event. Earlier during this event, both the WACR (Fig. 5a) and RWP (Fig. 5b) struggle to sample the thin and/or high cloud regions observed by ARSCL (Fig. 5c). CF estimates in these regions benefit from the additional ceilometer and MPL observations (not shown in Fig. 5) to detect clouds. Congestus clouds, including those having cloud tops ~6 km, are observed reasonably well by both radars. In these times, surface precipitation is limited (Fig. 5d). A deep convective cloud system passes over T3 between 1500-1900 UTC.

10 Heavy precipitation (surface measured rain rate  $> 60 \text{ mm h}^{-1}$ ) is associated with extinction of the WACR signal, whereas the RWP is able to reconstruct cloud boundaries up to 13 km. Since the RWP is sensitive only to precipitation-sized particles, these methods will still underestimate the true cloud top. Additional precipitation periods are also identified by red bars on top of Fig. 5c, highlighting locations where the cloud boundary designation within precipitation is improved over traditional ARSCL methods.

15

#### 2.4. Cloud Classification and Radiative Properties

A simple cloud-type classification is performed on the cloud boundary and masking dataset from Section 2.3. This approach follows McFarlane et al. [2013] and Burleyson et al. [2015]. These methods classify clouds into seven categories according to the height of the cloud boundaries and cloud thickness. The cloud categories include: shallow, congestus, deep

20 convection, altocumulus, altostratus, cirrostratus/anvil, and cirrus (definitions summarized in Table 1). Figure 5c provides an example of the cloud classifications for 1 April 2014. Cloud classification is used to separate surface radiative properties among the different cloud types. To accomplish this, the nearest cloud profile is matched to the 1-min surface radiative flux data. As with Burleyson et al. [2015], the lowest cloud type present in the column during that time is used to designate the shortwave and longwave radiative flux measurements (Figs. 5e and f) for that cloud type.

25

### 3. Profiling Observations of Clouds and Precipitation During GoAmazon2014/5

As highlighted in Fig. 2, thermodynamic and cloud properties from this two-year Amazon dataset are diverse and sampled near continuously by the ARM instrumentation to provide unique constraints towards model improvement. First, T3 cloud

observations will be summarized according to diurnal and seasonal breakdowns that follow from large-scale shifts between wet and dry Amazon precipitation regimes. Breakdowns of CF associated with each cloud category defined in the previous section are located in Table 2 (a variation of this Table is also found in Figs. 10 and 12). For composite CF summaries presented in this section, we capitalize on the high temporal and vertical resolution of the ARM instruments to partition CF according to hourly profile estimates.

Measurable precipitation (> 1 mm, daily) was frequent over the T3 site during the campaign according to surface rain gauge observations (as highlighted in Fig. 2b). In this dataset, 216 days recorded measurable precipitation from multiple ARM gauge and radar sensors, with eighty additional days recording light / trace precipitation (< 1 mm). The total campaign precipitation over T3 was approximately 3000 mm. This total T3 accumulation is representative of the regional SIPAM estimates reported in Zhuang et al. [2017], accounting for uncertainty in radar-based rainfall estimates, dataset gaps and discrepancies between point and spatial rainfall estimates. However, this total campaign precipitation may be below normal owing to a late onset of the 2014-2015 rainy season and other factors (e.g., Fig. 4 of Marengo et al. [2017], ~2300 mm/yr). Using collocated RWP echo classification methodologies when available (as described by Giangrande et al. [2016]), it was possible to designate the fractional precipitation associated with convective and stratiform regimes. For this dataset, ~76% of the accumulated precipitation was associated with convective precipitation. For this definition, we note that 'deep convective' cloud regimes from our cloud classification are associated with both convective precipitation in the convective cores that pass over the site, as well as stratiform precipitation in the case of trailing widespread precipitation regions behind the convective lines and mesoscale convective systems (MCSs, e.g., Houze et al. [2015]). Additional details on diurnal and regime breakdowns follow in the subsequent sections.

Deleted: cloud

### 3.1 Cloud and Precipitation Diurnal Cycles

Figure 6 shows diurnal CF profile breakdowns for each cloud category. The 'cirrus' and 'shallow' cloud categories are combined into a single panel since these cloud definitions do not overlap in altitude. Seasonal variations in the diurnal CF by cloud category are described in the next section. Figure 6a indicates that cirrus clouds are the most commonly observed clouds during the afternoon and overnight hours, whereas shallow cloud observations dominate the early morning hours after sunrise into the mid-afternoon. Combining Fig. 6a with summary cloud occurrence values in Table 2, shallow cumulus in the Amazon are observed with relatively high frequency throughout most of the day (~ 22%). Shallow clouds in the early morning align with low-level weak ascending air motions (Fig. 4a) and the positive advection of moisture (Fig. 4d). The most common cirrus clouds locations correspond to relatively high RH regions in the upper atmosphere seen in Fig. 4g, where the air is close to saturation with respect to ice (not shown).

Congestus (Fig. 6c) and deep convective (Fig. 6d) clouds are prominent ~~starting at noon into the late afternoon, with peak CF coverage an hour to two after local noon.~~ Deeper clouds that include ~~MCS passages~~ (identifiable using SIPAM observations) appear to maintain higher CFs into the overnight hours (associated with trailing stratiform regions). Integrated column behaviors are similar to those found from satellite over Manaus from Machado et al. [2004]; specifically, cloud coverage is high throughout the day, peaking after local noon and associated with increased cirrus (Fig. 6a), cirrostratus (Fig. 6b) and deeper convective clouds (Fig. 6d). The T3 location exhibits a pronounced diurnal cycle associated with deeper convection (as also in Saraiva et al. [2016]). This pronounced behavior is further representative of the fortuitous placement for the T3 AMF site, wherein daily cloud lifecycles also phase well with ~~propagating sea breeze intrusions over this portion of the Amazon basin [Burleyson et al. 2016].~~ ~~Primary diurnal peak~~ behaviors of these clouds (enhanced afternoon convection and reduced overnight convective development) ~~are associated with mid- and upper-level upward motion in the afternoon and downward air motion from night to the early morning (Fig. 4a).~~

~~Deleted:~~ during  
~~Deleted:~~ mid-to-  
~~Deleted:~~ around  
~~Deleted:~~ organized convective systems (

Congestus and altocumulus exhibit weak ~~peaks in the pre-dawn hours (around 0500 LT).~~ This is observed primarily as a wet season congestus behavior, possibly comparable to suggestions in previous Manaus diurnal rainfall efforts [e.g., Machado et al. 2004]. However, this contribution would typically be dwarfed when combining the rainfall contributions from other cloud types. We note that the non-precipitating categories of altocumulus, altostratus and cirrostratus (Figs. 6b, e, and f) share similar diurnal phasing with cirrus clouds. Cirrus and cirrostratus are more commonly observed than alto-cloud designations. However, we have not differentiated the contributions to cirrus CF estimates that reflect deep convective or anvil cloud components from other cirrus clouds. Overall, inspection of large-scale forcing fields supports that the diurnal cycle of high-level clouds is not well associated with the diurnal cycle of the large-scale dynamic and thermodynamics. This ~~may be~~ indicative ~~of the importance of~~ clouds that originate from anvil remnants from deeper convective clouds, ~~or advect from elsewhere, in addition to the clouds that are forced and developed locally.~~

~~Deleted:~~ rare  
~~Deleted:~~ D  
~~Deleted:~~ lign  
~~Deleted:~~ with

~~Deleted:~~ secondary

Figure 7 shows the diurnal cycle of precipitation properties at the T3 site as observed by the surface gauges collocated with RWP observations. These plots include wet, dry and transitional season contributions (although we do not isolate these transitional months). Average precipitation rates reflect the average across precipitating and nonprecipitating days, peaking around 1200 to 1600 LT (Fig. 7a), consistent with the deep convective CF in Fig. 6d. Note, the mean rainfall rates including only ~~days when precipitation is present (Fig. 7b)~~ are more comparable between wet and dry season events, suggesting T3 results in Fig. 7a primarily reflect the additional frequency of convection during the wet season and not its relative intensity. ~~The total rainfall accumulations for the various regimes are presented in Fig. 7c.~~ Rainfall ~~accumulations from Fig. 7c~~ have also been separated into convective and stratiform types as designated by the RWP ~~when available~~ [Giangrande et al. 2016]. For the composite campaign (dashed line in Fig. 7d), ~~convective precipitation is dominant at ~76% of the fractional accumulation (~2300 mm) with a relatively flat contribution diurnally (esp. during the dry season).~~ Since this fractional accumulation is based on RWP estimates for convective fraction, it may tend to maximize convective precipitation fraction

~~Deleted:~~ is  
~~Deleted:~~ of  
~~Deleted:~~ that developed locally  
~~Deleted:~~ ed  
~~Deleted:~~ .  
~~Deleted:~~

~~Deleted:~~ times

~~Deleted:~~ rates

~~Deleted:~~ c

over traditional scanning radar-based retrievals (e.g., Steiner et al. [1995]). This is because unlike basing these designations on radar reflectivity factor properties and buffering (proximity to convective cores based on intensity), profiler methods also distinguish columns with convective vertical air motions (including those from elevated, sloping updrafts that extend back into the transitional or trailing stratiform regions for MCSs), as well as congestus cloud precipitation (typically, associated with clouds having echo tops exceeding 4 km) as 'convective' rainfall. Stratiform precipitation (approx. 700 mm for this dataset) is more frequent (in terms of accumulation) during the overnight hours (30-60%) and is associated with the trailing precipitation regions from the convective systems. Again, based on our cloud classifications, 'deep convective' clouds would contain convective and widespread stratiform precipitation components.

Deleted: shallow

### 3.2 Seasonal Cloud Regime Cycles

Figure 7 also plots the diurnal breakdowns for average rainfall rate and fractional convective accumulations during the two wet and dry seasons over T3. Our dataset contains 103 wet season days responsible for approximately 1600 mm of precipitation, and 52 dry season days responsible for approximately 600 mm of precipitation. The wet season months are associated with a factor of 2 increase in mean rainfall rates, but even larger increases occur during daytime hours with much smaller changes during the late evening and early morning (Fig. 7a). However, relative to those days having precipitation (Fig. 7b), the differences in the mean rainfall rate are less pronounced. This may support that the dry season convection is stronger (instantaneously), since the overall convective cell coverage is also reduced during the dry season (e.g., Giangrande et al. [2016]; Schiro 2017). Wet and dry season convective rain fractions have similar values (~80%) throughout most of the day (Fig. 7d) and only diverge during the early morning hours when wet season convective rain fractions drop to as low as 20%. These diurnal patterns suggest that organized MCSs pass over T3 primarily in the morning hours during the wet season, but are infrequent and only have a small impact on the multi-month mean statistics.

Deleted: /stratiform

Deleted: hus,

Deleted: average

Deleted: ,

Deleted: imply

Deleted: ing

Deleted: as

Deleted: c

Deleted: systems

Figure 8 plots seasonal breakdowns for the CF diurnal cycle from Fig. 6 for the wet and dry seasons. Pronounced CF profile increases are associated with deep convective and congestus clouds during the wet season, with the dry season having less organized cloud contributions [Ghate and Kollias 2016]. Overnight and/or pre-dawn deep convection and additional local congestus development are more common in the wet season. The distinct nighttime enhancement in stratiform precipitation (once again, often categorized under "deep convection" in Figs. 6d, 8a and 8b) during the wet season is consistent with previous findings that propagating convective cloud systems contribute to the observed diurnal cycle of deep convection [e.g., Burleyson et al. 2016, Tang et al. 2016]. Early morning shallow cumulus CF profiles (Figs. 8a and 8b) indicate frequent low clouds during wet and dry seasons, consistent with a response to increased surface heating and an increase in the surface latent heat flux, with the wet season reporting additional shallow cloud development throughout the diurnal window (and the dry season consistent with elevated LCL heights). Two separate vertical peaks of shallow cumulus CF were observed between predawn and early morning hours (0300-0900 LT) during the wet season: one right above the surface, and

Deleted: s

Deleted: and 9

Deleted: , respectively

Deleted: (e.g., organized, continuation)

Deleted: identified

Deleted: as

Deleted: D

Deleted: C

Deleted: d and 9d

Deleted: s

Deleted: a and 9a

the other at 2 km height. The surface peak is possibly associated with overnight fog being lifted with surface heating associated with the rising sun [e.g., Anber et al. 2015], while the elevated peak may be associated with radiative cooling of the residual boundary layer overnight. Cirrus CF stays elevated during the wet and dry seasons, however cirrostratus/anvil CFs are substantially reduced during the dry season. This pattern suggests mostly a local deep convective contribution to cirrostratus/anvil during the dry season, with local convection and potentially some additional remnant anvil or decaying MCS cloud components advected over T3 during overnight hours under wet season conditions. Quantitative interpretation for these behaviors is challenging owing to coupled cirrus-shallow cloud sampling factors during the overnight hours. For example, it is likely cirrus sampling is shielded (results stemming from an MPL detection) during the wet season owing to the added presence of lower-level clouds and higher relative humidity / attenuation limiting the usefulness of the cloud radar.

In contrast, clear low-level conditions during the overnight hours of the dry season would likely promote improved designation of cirrus. In this regard, wet and dry season cirrus cloud contrasts may be more pronounced than reported by this study.

Deleted: (cf. Figs. 8b and 9b)

Deleted: o

Deleted: rganized

As highlighted by Figs. 2 and 3, wet season thermodynamical conditions typically favor weaker CAPE, weaker CIN and higher RH in the lower to mid-atmospheric levels, while dry seasons feature stronger CAPE, stronger CIN and lower RH at the same levels. As inferred from the large-scale forcing fields in Fig. 4, wet season conditions favor higher column relative humidity, as well as heightened moisture convergence throughout the profile. The wet season also features more favorable omega fields at mid-levels for shallow to deeper convective cloud transitions. This behavior is not surprising and also consistent with forcing datasets being constrained using mean domain precipitation estimates. However, as with first year GoAmazon2014/5 studies (e.g., Collow et al. [2016]), only weak correlations are found between cloud state, and thermodynamic parameters (not shown). Nevertheless, coupled thermodynamical and environmental forcing conditions from Section 2 support these observations of more frequent cloudiness during the wet season, visible across almost all cloud categories (Fig. 8).

Deleted: behaviors

Deleted: when comparing Fig. 8 to Fig. 9

### 3.3 Comparison of Cloud Observations with Satellite: Shallow Cumulus Representativeness

An important consideration when interpreting ARM T3 observations is the spatiotemporal representativeness of the cloud fractions over T3 within this central Amazon region. Satellite observations provide one avenue to better understand the representativeness of the location, while also providing insights into the advantages afforded by ground-based ARM cloud observations. Several recent GoAmazon2014/5 studies including Burleyson et al. [2016] and Giangrande et al. [2016] have investigated the representativeness of the T3 site as compared to satellite and/or radar perspectives. In these studies, they found evidence suggesting that T3 observed deep convection are well-correlated with the regional cloud and precipitation to within a few hundred kilometers of the site. As a complementary reference, we approach the topic from a shallow cumulus

perspective, as these clouds provide some of the better ground and aircraft-based datasets opportunities collected during this campaign.

Figure 9 provides a diurnal comparison plot of shallow cumulus cloud fraction between T3 ground-based estimates, the Geostationary Operational Environmental Satellite (GOES) SatCORPS (Minnis et al. [2011]) and the Moderate Resolution Imaging Spectroradiometer (MODIS, Platnick et al. [2003]) products for wet and dry seasons (comparisons performed between February and December of 2014 when both satellite datasets are available). Both satellite cloud products are based on multi-channel passive sensors onboard, providing fundamentally different cloud detection techniques compared to active sensors at T3. We chose these satellite data products because they provide large area coverage and frequent updates, making the comparison with single-point surface observations more amenable. The cloud property retrievals are available at 4 km spatial and 30-min temporal resolution for GOES, and at 1 km spatial and two overpasses during ~10:30 LT and ~13:30 LT for MODIS. Shallow cumulus clouds are defined as pixel-level cloud-top height below 3 km, consistent with T3 ground-based definitions. Shallow cumulus cloud fractions are then calculated at several spatial coverage domains (from 25 km to 150 km) for GOES, and at 25 km domain for MODIS. We find that the GOES mean CF estimates are similar in their diurnal cycle and magnitude as a function of the domain size, with increasing variability in CF estimates (shadings) to the smaller domain sizes. The MODIS mean CF estimates are higher than those obtained from GOES, but share similar diurnal patterns and ranges of variability as to the GOES smaller domain estimates.

In comparison with the satellite observations, single-point T3 ground estimates of shallow cumulus are the largest and carrying the largest observational spread, but demonstrate diurnal and peak behaviors that are roughly comparable to the satellite counterparts. Discrepancies in CF estimate (mean) magnitude are not surprising, with the largest discrepancies found in the wet season. These differences may be related to several factors including the obscured view of shallow cloud from passive satellite retrievals, for example owing to the blockage from higher clouds (i.e., multi-layer clouds). Moreover, over the entire field campaign period, single layer clouds occur ~48% of the time, while multi-layer clouds occur ~20% of the time. During the wet seasons, multi-layer clouds occur twice as often as during the dry seasons (~28% vs. ~11%). The coarser resolution and/or sensitivity of the satellite platforms to shallower cumulus may also contribute to the lower mean CF values. The higher resolution MODIS product shows higher shallow cumulus CF estimates than GOES during MODIS overpass times, demonstrating additional benefits of increased resolution in detecting shallow cumulus clouds, especially compared to ground-based active remote sensing observations. Finally, unavoidable discrepancies and variability still may trace to spatial domain versus column-temporal CF definition differences (e.g., Berg and Stull [2002]) or factors including localized circulations generated by river breezes (e.g., Burleyson et al. [2016]). Overall, this shallow cumulus comparison between T3 ground-based and satellite observations suggests that mean cloud fractions near the T3 location should be representative of larger domain cloud properties to within a few hundred kilometers.

- Formatted: Font:Not Bold

Deleted: .

#### 4. Cloud Type Influence on Surface Energy and Fluxes

AMF instrumentation provides unique capabilities to characterize the variability of clouds and their impact on the Amazon surface energy budget (e.g., Collou and Miller [2016]). Previously, Burleyson et al. [2015] quantified the diurnal cycle of surface cloud radiative effects (CRE) over the three ARM sites in the Tropical Western Pacific (TWP, e.g., Long et al. [2016], ARM [2013]) using long term measurements of ARSCL cloud profiles and surface radiative flux analysis. CRE is defined as cloudy-sky downwelling flux minus clear-sky downwelling flux. By breaking down the aggregate surface CRE by cloud type across the diurnal cycle, Burleyson et al. [2015] found that the largest source of shortwave surface CRE at these three TWP sites comes from low clouds owing to their high frequency of occurrence. Although deep convective clouds have a strong influence on surface shortwave radiation when present, their aggregate impact is limited by a lower frequency of occurrence compared to shallow cumulus. Longwave CRE is typically a factor of 5-6 smaller than SW CRE [e.g., Culf et al. 1998; Malhi et al. 2002, Burleyson et al. 2015]. This study will limit most interpretation to SW CRE. The 2-year deployment during GoAmazon2014/5 allows us to examine the impact of various cloud types on the surface energy budget over the Amazon, providing new details for targeted model improvements of cloud radiative effects in this climatically important, but undersampled region. This deployment also provides a unique opportunity to contrast ‘green ocean’ cloud radiative effects during GoAmazon2014/5 with tropical ARM fixed-site measurements in the TWP.

Deleted: Compared to SW CRE,

Deleted: W

The frequency of occurrence for the lowest cloud types and their associated radiative fluxes (Tables 2 and 3) are composited into hourly bins across the diurnal cycle (Fig. 10). Table 3 is also complemented by Fig. 11, to better illustrate the diurnal cycle of those mean values and their variability for the complete record and including wet/dry season breakdowns. The methodology to produce the radiative fluxes in these tables is similar to Burleyson et al. [2015] to facilitate comparison with previous results over the three TWP sites. We utilize ‘as lowest cloud type’ in the column designations in our analysis (e.g., column 2 in Table 2) because clouds closest to the surface typically have the larger impact on the surface radiative fluxes [Burleyson et al. 2015]. However, we also note that it is not possible to separate the radiative impact of multi-layer clouds and sample sizes are potentially too small to only consider single-layer cloud periods. For higher-altitude cloud types, the frequency as lowest cloud in the column is lower than the total cloud frequencies discussed in Section 3 (as reported in column 1 of Table 2). The difference in frequencies is indicative of how often multi-layer clouds are present (e.g., cirrus clouds are often present above shallow cumulus).

Deleted: 0

One notable discrepancy with the previous study is that the instrumentation for classifying the clouds that produce significant precipitation (rain-rate  $> 1 \text{ mm h}^{-1}$ ) during GoAmazon2014/5 is better than the approach used by Burleyson et al. [2015] owing to the merging of the RWP dataset. Specifically, cloud profiles with rain-rate larger than  $1 \text{ mm h}^{-1}$  are discarded in Burleyson et al. [2015], but retained for our study. Therefore, we anticipate that cloud radiative effects from

precipitating convective clouds (including both congestus and deep convection) may be more accurate than Burleyson et al. [2015].

Deleted: are better represented by this study

#### 4.1. Bulk Cloud Radiative Effects

- 5 The average aggregated shortwave (SW) and longwave (LW) fluxes, and CRE measured at the T3 site are given in Table 3, along with long term results from the three TWP sites (Darwin, Manus, Nauru) as reported in Burleyson et al. [2015]. SW CRE dominates (magnitude) as compared to LW CRE. The mean SW CRE ( $-94.4 \text{ W m}^{-2}$ ) and LW CRE ( $14.5 \text{ W m}^{-2}$ ) averaged across the diurnal cycle (nighttime included) over the entire GoAmazon2014/5 is most similar to those found at Manus, which is the cloudiest of the three TWP sites and most influenced by convection in the Western Pacific warm pool.
- 10 The Darwin, Australia site has a strong monsoonal cycle (i.e., wet/dry season) and the Nauru site is strongly impacted by the El Niño–Southern Oscillation (ENSO) variability [Burleyson et al. 2015]. Manus would be the one most qualitatively consistent with the GoAmazon2014/5 ‘green ocean’ moniker. During the wet season, SW CRE ( $-121.5 \text{ W m}^{-2}$ ) is twice the dry season value ( $-60.4 \text{ W m}^{-2}$ ), although CREs for this region of the Amazon basin are substantially larger than Darwin during all seasons. However, although mean behaviors initially appear similar, the properties from individual cloud types are not necessarily consistent between, for example, Manus and Manaus (e.g., see Burleyson et al. [2015] Table 4). A more thorough breakdown of the factors driving these specific differences (e.g., the time of day when a given cloud type is more or less prevalent, the frequency of multi-layer clouds, or variance in the clear sky downwelling SW or LW flux) is recommended as a future activity from these GoAmazon2014/5 datasets.
- 15
- 20 Table 2 gives bulk cloud frequency and their radiative characteristics separated by cloud types and by season. The results reveal the averaged reduction of downwelling SW flux when a particular cloud type is present. Consistent with the SW transmissivity results (Table 2) and those found by Burleyson et al. [2015], congestus and deep convective clouds dominate the conditional (e.g., not a mean property) SW CRE, while cirrus clouds have the smallest effect on downwelling SW flux. Note, the conditional CRE presented in Table 2 includes both single-layer clouds, as well as when additional cloud layers are
- 25 above the lowest detected cloud layer. This is done deliberately to be consistent with the method used by Burleyson et al. [2015] such that the GoAmazon2014/5 results can be directly compared with their long-term results from the ARM TWP sites. Examination of the averaged conditional SW CRE calculated using only single-layer clouds reveal a relative reduction of ~26% for altocumulus and ~20% for shallow cumulus clouds, and negligible difference in other cloud types. The reduction in SW CRE when single-layer clouds are considered is likely caused by frequent multi-layer cloud occurrence of
- 30 cirrus/cirrostratus clouds over shallow cumulus or altocumulus (i.e., artificially inflating the surface SW CRE of cumulus clouds due to additional SW flux reflection by the upper level clouds). The difference in conditional SW CRE between single- and multi-layer clouds do not change their contribution to the average CRE as discussed below.

Deleted: ,

Deleted: 15

Deleted: 6

Deleted: 54

Deleted: 9

#### 4.2. Diurnal Cycle of Cloud Radiative Effects by Cloud Type

Comparisons between wet and dry season diurnal behaviors for the frequency of the lowest clouds in the column and the associated mean SW CRE are shown in Fig. 12. Shallow cumulus dominates the SW CRE in both seasons, although their frequency peak two hours earlier during wet season (1000-1100 LT) than during dry season (1200-1300 LT). While the dry season features reduced frequency and SW CRE of all cloud types, the contrast is most visible for the three convective cloud types. Shallow, congestus and deep convective cloud mean SW CRE in the wet season are 50%, 69% and 72% larger than that in the dry season, respectively (their mean SW CRE values across the diurnal cycle are shown in Fig. 12c, 12d).

Deleted: 1

Deleted: 1

Deleted: 1

#### 4.3. Shallow Cumulus Cloud Properties

From the previous section, shallow cumulus (those most frequently observed during the campaign) are associated with large discrepancies in cloud radiative effects between the wet and dry season (Table 2 and Fig. 13). Further investigation into these clouds and their radiative differences is enabled using aircraft observations available during the GoAmazon2014/5 campaign IOP periods. As discussed in Section 2.2, three cloud particle size distribution probes are combined to create the full DSD (Fig. 13). Combining the cloud microphysical properties in shallow cumulus measured by aircraft observations and the cloud macrophysical properties measured by ground-based instrumentations allow us to explain the cloud radiative effect differences from wet and dry seasons reported in the previous section.

Deleted: 11

Deleted: 2

Cloud particle size distributions (Fig. 13e) in the wet season are characterized by a lesser occurrence of small droplets and a more frequent occurrence of large droplets when compared with cumulus clouds in the dry season. Total number concentration of cloud drops is more than a factor of 2 larger in the dry season versus the wet season (Fig. 13b). However, the corresponding LWC is roughly the same between the seasons (Fig. 13d). In-situ cloud condensation nuclei (CCN) concentration is also larger in the dry season versus the wet season (Fig. 13a). Aircraft cloud and CCN measurements are consistent with studies that show clouds influenced by aerosol tend to have larger concentrations of smaller droplets and fewer precipitation sized drops for clouds with similar LWC [e.g., Twomey 1974; Cecchini et al. 2016]. Ground-based radar measurements of single layer shallow cumulus clouds at the T3 site show thicker clouds occurring more frequently in the wet season (Fig. 13e). Likewise, more frequent occurrence of large liquid water path (LWP) from the T3 ground-based MWR in wet season is consistent with the presence of more robust (i.e., vertically developed) shallow cumulus clouds (Fig. 13f). Therefore, shallow cumulus in the wet season is characterized by fewer number but more frequent larger cloud droplets, while those in the dry season is characterized by more frequent smaller cloud droplets (Fig. 13b,c). Interestingly, these differences in DSDs result in comparable LWC between the wet/dry seasons (Fig. 13d). As a result, the stronger

Deleted: 2

shallow cumulus conditional SW CRE in the wet season, which reflects the difference in microphysical properties, mainly arises from higher values of vertically integrated properties such as LWP and cloud thickness (Fig. 13e,f).

Deleted: 2

## 5. Discussion, Summary and Future Opportunities

Deleted: Column Break

5 This study documents the continuous observations collected by the DOE AMF and AAF facilities to characterize cloud properties, collocated large-scale environments and cloud radiative effects over the two-year GoAmazon2014/5 campaign. This extended ground deployment included high temporal and vertical resolution cloud profiling instrumentation, enabling a unique perspective on various cloud types and their diurnal evolution to complement previous satellite-based perspectives over this undersampled region. Routine thermodynamic profiling over the diurnal cycle, targeted IOP aircraft sampling, and collocated aerosol instrumentation support future opportunities to differentiate and interpret cloud lifecycle and process factors influenced by environmental forcing controls and those influenced by coupled cloud-aerosol interactions within pristine and polluted conditions [e.g., Martin et al. 2017]. [Analysis performed in this study and by previous GoAmazon2014/5 works \[Burleyson et al. 2016; Giangrande et al. 2016\] suggest that both shallow cumulus and deep convection observed over the AMF site are representative of larger domain cloud properties to within a few hundred kilometers. These studies indicate the usefulness of the datasets collected during the campaign to enable future studies to better understand the forcing control of the diurnal cycle, seasonal variability of clouds in the central Amazon region and associated feedbacks to the climate system.](#)

20 The propensity for cumulus to initiate, deepen and organize across the Amazon basin drives much of the observed wet and dry season CF profile diurnal contrasts. Amazon wet season environments promote enhanced shallow cumulus throughout the diurnal cycle, as well as additional deeper precipitating cloud development likely associated with reduced CIN, heightened moisture convergence and relative humidity through atmospheric mid-levels. Wet season and transitional periods exhibiting sharper CAPE and CIN contrasts [potentially](#) enhance the likelihood for deep convection to [develop](#), promoting anvil and trailing stratiform regions that carry into the overnight hours and propagate across the Amazon basin. Weaker secondary peaks in congestus CFs are also found during the wet season within pre-dawn hours, revealed with confidence from coupled ARM profiling observations. Nevertheless, relatively favorable thermodynamical conditions during both seasons supports local congestus [and deeper cloud formation](#), for this ARM dataset, which includes over 200 days recording measurable rainfall. This regularly occurring daily precipitation is primarily attributed to isolated and locally-driven convective cells, supported by the 76% rainfall accumulation associated with convective modes, as well as the pronounced diurnal cycle for this rainfall centered near local noon. These ideas and [the representativeness of the T3 measurements for](#)

Deleted: have organized components

Deleted: thus

Deleted: to

Deleted: triggering

Deleted: representativeness

cloud studies beyond examples presented within this study for shallow cumulus may be further explored using spatial observations, as available from collocated SIPAM radar observations during GoAmazon2014/5

**Deleted:** properties

5 Congestus and deeper convection is also shown to dominate the conditional surface SW CRE, similar to results from previous tropical ARM analyses over the TWP region. As one possible example for the appropriateness of the Amazon 'green ocean' moniker, mean CRE properties for the Amazon are found to be similar to the TWP ARM Manus location in the Western Pacific warm pool that favors frequent tropical convection with complex influences from adjacent large islands within the Maritime Continent [e.g., Mather 2005]. However, a more thorough analysis is recommended, as these similarities in mean CRE properties do not always hold for individual cloud types. Similarly, a natural contrast between Amazon SW  
10 CRE behaviors and those from ARM Nauru observations stems from the strong ENSO-driven variability over this site as a key driver for cloud coverage [e.g., Jensen et al. 1998, Burleyson et al. 2015]. The cumulative Amazon CRE is also larger when compared to the Darwin wet season (given the 'dry' season for Darwin is void of substantial cloud/precipitation). This behavior is partially attributed to the Darwin monsoonal environments that fluctuate between wider-spread tropical 'Active' cloud conditions and continental 'Break' monsoonal regimes that promote stronger convection [e.g., Holland 1986; May and  
15 Ballinger 2007; Giangrande et al. 2014]. Overall, cumulative results from CRE help emphasize the important role of shallow cumulus for the Amazon, including the dry season, and the favorable low-level conditions (e.g., weak ascending air motions, positive moisture advection and moist surface) throughout the year that promote elevated shallow cumulus frequency. Given this relative importance, these clouds must be properly simulated in both global and regional climate models if the surface radiative budget (that affects land-atmosphere interactions and subsequent convective cloud and precipitation formations  
20 over the T3 site) is to be properly represented.

**Deleted:** efforts

**Deleted:** A

Ground-based multi-sensor measurements and aircraft observations further support thicker cumulus clouds occurring more frequently in the wet season. These clouds are those having larger LWP that would also promote the heightened SW CRE and LW CRE contributions. Aircraft and ground-based cloud and CCN measurements and properties for shallow cumulus in  
25 this study also informs on the role of the Manaus pollution plume in cumulus cloud evolution. A key motivation behind GoAmazon2014/5 was the opportunity to test various cloud-aerosol interactions in the Amazon. Shallow cumulus summaries provided in our study are consistent with the hypothesis that clouds influenced by aerosol tend to have a larger concentration of smaller droplets and fewer precipitation sized drops for clouds with similar LWC. As the clean (wet) and  
30 polluted (dry) cloud conditions tend to align with large-scale regime thermodynamical controls, subsequent studies will need to differentiate the role of the Manaus plume that influences the observed differences in shallow cumulus microphysical properties, and examine the extent that the reduced frequency for MCSs removes Manaus pollution. In that regard, impacts on shallow cumulus clouds could have potentially a more profound impact as far as how shallow clouds transition to deeper convection, hence affecting hydrological cycle and land-atmosphere feedbacks.

**Deleted:** is

**Deleted:** natural cloud laboratory setting

**Formatted:** Font:(Default) +Theme Body (Times New Roman)

**Formatted:** Font:(Default) +Theme Body (Times New Roman), 10 pt

**Formatted:** Font:(Default) +Theme Body (Times New Roman), 10 pt

**Formatted:** Font:(Default) +Theme Body (Times New Roman)

**Deleted:** support prior efforts that suggest clouds influenced by aerosol tend to have larger concentrations of smaller droplets and fewer precipitation sized drops for clouds with similar LWC.

**Deleted:** organized precipitation

**Deleted:** events

## 6. Data Availability

All ARM datasets used for this study may be downloaded at <http://www.arm.gov>, and associated with several “Value Added Product” streams (e.g., ARM Climate Research Facility, 1993;2005; 2009;2013). MODIS Aqua and Terra, level L2, collection 6, cloud property data with 1 km resolution are obtained from NASA’s Distributed Active Archive Centers (DAACs) <https://earthdata.nasa.gov/about/daacs>. These data are parts of the NASA Earth Observing System Data and Information System (EOSDIS) managed by the NASA Earth Science Data and Information System (ESDIS) project. Cloud properties (including effective cloud top heights) from the Thirteenth Geostationary Operational Environmental Satellite (GOES-13) were derived via SatCORPS (Satellite Cloud Observations and Radiative Property retrieval System), a suite of algorithms including the 4 channel VISST (Visible Infrared Solar-Infrared Split-Window Technique) daytime algorithm, and nighttime 3 channel SIST (Solar-infrared Infrared Split-Window Technique) and SINT (Solar-infrared Infrared Near-Infrared Technique), versions similar to those described by Minnis et al. [2011]. This cloud and radiative property dataset with 4 km resolution (v4.1) was processed for the GoAmazon 2014/5 domain covering 3°N-10°S, 50°W-70°W. It was obtained from mid-February through December 2014, from the NASA Langley Research Center Cloud and Radiation Research Group (<https://satcorps.larc.nasa.gov/ARM-GOAMAZON>). A subset of this dataset, covering the AMF and local vicinity (5°×5°), can be obtained from the ARM archive.

## 7. Acknowledgements

This manuscript has been authored by employees of Brookhaven Science Associates, LLC under Contract No. DE-SC0012704 with the U.S. Department of Energy (DOE). The publisher by accepting the manuscript for publication acknowledges that the United States Government retains a non-exclusive, paid-up, irrevocable, world-wide license to publish or reproduce the published form of this manuscript, or allow others to do so, for United States Government purposes. Dr. Zhe Feng at the Pacific Northwest National Laboratory (PNNL) is supported by the U.S. DOE, as part of the Atmospheric System Research (ASR) Program. The PNNL is operated for DOE by Battelle Memorial Institute under contract DE-AC05-76RL01830. Work at the Lawrence Livermore National Laboratory (LLNL) was supported by the DOE ARM program and performed under the auspices of the U.S. DOE by LLNL under contract No. DE-AC52-07NA27344. Funding was also obtained from the U.S. DOE, the São Paulo Research Foundation (FAPESP - 2009/15235-8), The Amazonas State University (UEA) and the Amazonas Research Foundation (FAPEAM - 062.00568/2014). The work was conducted under scientific licenses 001030/2012-4, 001262/2012-2, and 00254/2013-9 of the Brazilian National Council for Scientific and Technological Development (CNPq). Institutional support was provided by the Central Office of the Large Scale Biosphere

Atmosphere Experiment in Amazonia (LBA), the National Institute of Amazonian Research (INPA), the National Institute for Space Research (INPE), and the Brazil Space Agency (AEB). We also acknowledge the Atmospheric Radiation Measurement (ARM) Climate Research Facility, a user facility of the U.S. DOE, Office of Science, sponsored by the Office of Biological and Environmental Research, and support from the ASR program of that office. [The authors thank the three anonymous reviewers for their constructive comments to improve the manuscript.](#) Additional thanks to Mark Miller (Rutgers University) for an internal review of this manuscript. Thanks also to support from Duli Chand and Mandy Thieman for satellite datasets. The GoAmazon2014/5 GOES-13 satellite retrievals were also supported by the U.S. Department of Energy, Office of Biological and Environmental Research, Atmospheric System Research Program award DE-SC0000991.

## References

Ackerman, T. P., and G. M. Stokes, 2003: The Atmospheric Radiation Measurement Program, *Physics Today*, 39-44.

Alcântara, C. R., Dias, M. A.F. Silva, Souza, E. P., Cohen, J. C.P.. 2011. Verification of the role of the low level jets in Amazon squall lines. *Atmospheric Research* (Print), v.100, 36-44

Anber, U., P. Gentine, S. G. Wang, and A. H. Sobel (2015), Fog and rain in the Amazon, *Proc. Natl. Acad. Sci. U. S. A.*, 112 (37), 11,473 – 11,477.

Atmospheric Radiation Measurement (ARM) Climate Research Facility. 1993, updated hourly. Balloon-Borne Sounding System (SONDE). 3.21297 S 60.5981 W: ARM Mobile Facility (MAO) Manacapuru, Amazonas, Brazil; AMF1 (M1). Compiled by D. Holdridge, J. Kyrouac and R. Coulter. Atmospheric Radiation Measurement (ARM) Climate Research Facility Data Archive: Oak Ridge, Tennessee, USA. Data set accessed at <http://dx.doi.org/10.5439/1025284>

Atmospheric Radiation Measurement (ARM) Climate Research Facility. 2005, updated hourly. W-Band (95 GHz) ARM Cloud Radar (WACR). 3.21297 S 60.5981 W: ARM Mobile Facility (MAO) Manacapuru, Amazonas, Brazil; AMF1 (M1). Compiled by N. Bharadwaj, D. Nelson, B. Isom, J. Hardin, I. Lindenmaier, K. Johnson and A. Matthews. Atmospheric Radiation Measurement (ARM) Climate Research Facility Data Archive: Oak Ridge, Tennessee, USA. Data set accessed at <http://dx.doi.org/10.5439/1025317>

Atmospheric Radiation Measurement (ARM) Climate Research Facility (2009), Updated hourly, Radar Wind Profiler (1290RWPPRECIPMOM). Compiled by R. Coulter, T. Martin and P. Muradyan. Atmospheric Radiation Measurement (ARM) Climate Research Facility Data Archive: Oak Ridge, Tenn. [Available at 10.5439/1025128.]

5  
Atmospheric Radiation Measurement (ARM) Climate Research Facility. 2013, updated hourly. Radiative Flux Analysis (RADFLUX1LONG). 2014-01-01 to 2015-12-31, ARM Mobile Facility (MAO) Manacapuru, Amazonas, Brazil; AMF1 (M1). Compiled by C. Long, K. Gaustad and L. Riihimaki. Atmospheric Radiation Measurement (ARM) Climate Research Facility Data Archive: Oak Ridge, Tennessee, USA. Data set accessed at <http://dx.doi.org/10.5439/1157585>.

10  
Bedacht, E., S. K. Gulev, and A. Macke (2007), Intercomparison of global cloud cover fields over oceans from the VOS observations and NCEP/NCAR reanalysis, *Int. J. Climatol.*, 27, 1707–1719, doi:10.1002/joc.1490.

Berg, L. K., and R. B. Stull, 2002: Accuracy of point and line measures of boundary layer cloud amount. *J. Appl. Meteor.*,  
15 41, 640 – 650.

Betts, A. K., J. Fuentes, M. Garstang, and J. H. Ball, (2002): Surface diurnal cycle and Boundary Layer structure over Rondonia during the rainy season, *J. Geophys. Res.*, 107, 8065, doi:10.1029/2001JD000356.

20 [Bunkers, M., B. Klimowski, and J. W. Zeitler, 2002: The importance of parcel choice and the measure of vertical wind shear in evaluating the convective environment. Extended Abstracts, 21st Conf. on Severe Local Storms, San Antonio, TX, Amer. Meteor. Soc., P8.2. \[Available online at \[http://ams.confex.com/ams/SLS\\\_WAF\\\_NWP/techprogram/paper\\\_47319.htm\]\(http://ams.confex.com/ams/SLS\_WAF\_NWP/techprogram/paper\_47319.htm\).\]](#)

Burleyson, C.D., C. N. Long, and J. M. Comstock. (2015), Quantifying Diurnal Cloud Radiative Effects by Cloud Type in  
25 the Tropical Western Pacific. *Journal of Applied Meteorology and Climatology* 54:6, 1297-1312.

Burleyson, C. D., Z. Feng, S. M. Hagos, J. Fast, L. A. T. Machado, and S. T. Martin, 2016: Spatial Variability of the Background Diurnal Cycle of Deep Convection around the GoAmazon2014/5 Field Campaign Sites. *J. Appl. Meteor. Climatol.*, doi:10.1175/JAMC-D-15-0229.1.

30  
Cecchini, M. A., Machado, L. A. T., Comstock, J. M., Mei, F., Wang, J., Fan, J., Tomlinson, J. M., Schmid, B., Albrecht, R., Martin, S. T., and Artaxo, P.: Impacts of the Manaus pollution plume on the microphysical properties of Amazonian warm-phase clouds in the wet season, *Atmos. Chem. Phys.*, 16, 7029-7041, doi:10.5194/acp-16-7029-2016, 2016.

Deleted: .

- Cohen, J. C. P., Silva Dias, M.A.F., Nobre, C. A. 1995. Environmental Conditions Associated With Amazonian Squall Lines: A Case Study. *Monthly Weather Review*, v.123, 3163-3174
- Collow, A. B., M., M. A. Miller, and L. C. Trabachino (2016), Cloudiness over the Amazon rainforest: Meteorology and thermodynamics, *J. Geophys. Res. Atmos.*, 121, 7990–8005, doi:10.1002/2016JD024848.
- Collow, A. B., and M. A. Miller, 2016: The Seasonal Cycle of the Radiation Budget and Cloud Radiative Effect in the Amazon Rain Forest of Brazil. *J. Climate.*, DOI: <http://dx.doi.org/10.1175/JCLI-D-16-0089.1>
- 10 Comstock, J. M., T. P. Ackerman, and G. G. Mace, 2002: Groundbased lidar and radar remote sensing of tropical cirrus clouds at Nauru Island: Cloud statistics and radiative impacts. *J. Geophys. Res.*, 107, 4714, doi:10.1029/2002JD002203.
- Clothiaux, E. E., T. P. Ackerman, G. G. Mace, K. P. Moran, R. T. Marchand, M. A. Miller, and B. E. Martner (2000), Objective determination of cloud heights and radar reflectivities using a combination of active remote sensors at the ARM  
15 CART sites, *J. Appl. Meteorol.*, 39, 645.
- Culf, A. D., G. Fisch, J. Lean, and J. Polcher, 1998: A comparison of Amazonian climate data with general circulation model simulations. *J. Climate*, 11, 2764–2773, doi:10.1175/1520-0442(1998)011<2764:ACOACD>2.0.CO;2.
- 20 Del Genio, A.D., 2012: Representing the sensitivity of convective cloud systems to tropospheric humidity in general circulation models. *Surv. Geophys.*, 33, 637-656, doi:10.1007/s10712-011-9148-9.
- Dos Santos, M. J., M.A. F. Silva Dias, E. D. Freitas, 2014. Influence of local circulations on wind moisture and precipitation close to Manaus City, Amazon Region – Brazil. *Journal of Geophysical Research* 119, (23), 13,233-13,249  
25 doi:10.1002/2014JD021969.
- Dupont, J.-C., M. Haeffelin, Y. Morille, J. M. Comstock, C. Flynn, C. N. Long, C. Sivaraman, and R. K. Newson, 2011: Cloud properties derived from two lidars over the ARM SGP site. *Geophys. Res. Lett.*, 38, L08814, doi:10.1029/2010GL046274.
- 30 Feng, Z., X. Q. Dong, and B. K. Xi, 2009: A Method to Merge WSR-88D Data with ARM SGP Millimeter Cloud Radar Data by Studying Deep Convective Systems. *J. Atmos. Oceanic Technol.*, 26, 958-971.

- Feng, Z., S. A. McFarlane, C. Schumacher, S. Ellis, J. Comstock, and N. Bharadwaj, 2014: Constructing a Merged Cloud-Precipitation Radar Dataset for Tropical Convective Clouds during the DYNAMO/AMIE Experiment at Addu Atoll. *J. Atmos. Oceanic Technol.*, **31**, 1021-1042.
- 5 Fisch, G.; Tota, J.; Machado, L. A. T.; Silva Dias, M. A. F.; Lyra, R. F. D.; Nobre, C. A.; Dolman, A. J.; Gash, J. H. C. The convective boundary layer over pasture and forest in Amazonia. *Theoretical and Applied Climatology*, v. 78, n. 1-3, p. 47-59, Jun. 2004. (INPE-11144-PRE/6600).
- Fu, R., and W. Li, 2004: Influence of land surface on transition from dry to wet season over the Amazonia. *Theor. Appl. Climatol.*, **78**, 97–110.
- 10 Fu, R., and B. Zhu, R Dickinson, 1999: How do the atmosphere and land surface influence the seasonal changes of convection in tropical Amazon? *J Climate* 12: 1306–1321
- 15 Ghate, V.P., and P. Kollias, 2016: On the Controls of Daytime Precipitation in the Amazonian Dry Season. *J. Hydrometeorol.* DOI: <http://dx.doi.org/10.1175/JHM-D-16-0101.1>
- Giangrande, S. E., E. P. Luke, and P. Kollias, 2012: Characterization of vertical velocity and drop size distribution parameters in widespread precipitation at ARM facilities. *J. Appl. Meteor. Climatol.*, **51**, 380–391.
- 20 Giangrande, S. E., S. Collis, J. Straka, A. Protat, C. Williams, and S. Krueger, 2013: A summary of convective-core vertical velocity properties using ARM UHF wind profilers in Oklahoma. *J. Appl. Meteor. Climatol.*, **52**, 2278–2295, doi:10.1175/JAMC-D-12-0185.1.
- 25 Giangrande, S. E., M. J. Bartholomew, M. Pope, S. Collis, and M. P. Jensen, 2014: A summary of precipitation characteristics from the 2006–11 northern Australian wet seasons as revealed by ARM disdrometer research facilities (Darwin, Australia). *J. Appl. Meteor. Climatol.*, **53**, 1213–1231
- 30 Giangrande, S. E., T. Toto, M. P. Jensen, M. J. Bartholomew, Z. Feng, A. Protat, C. R. Williams, C. Schumacher, and L. Machado (2016), Convective cloud vertical velocity and mass-flux characteristics from radar wind profiler observations during GoAmazon2014/5, *J. Geophys. Res. Atmos.*, 121, 12,891–12,913, doi:10.1002/2016JD025303.

- Holland, G. J., 1986: Interannual variability of the Australian summer monsoon at Darwin: 1952–82. *Mon. Wea. Rev.*, **114**, 594–604.
- Houze, R. A., K. L. Rasmussen, M. D. Zuluaga, and S. R. Brodzik, 2015: The variable nature of convection in the tropics and subtropics: A legacy of 16 years of the Tropical Rainfall Measuring Mission satellite. *Rev. Geophys.*, **53**, 994-1021.
- Jensen, M. P., J. H. Mather and T. P. Ackerman, 1998: Observations of the 1997-98 warm ENSO event at the Manus Island ARM site. *Geophys. Res. Lett.*, **25** (24), 4517-4520.
- 10 Jensen, M. P., T. Toto, D. Troyan, P. Ciesielski, D. Holdridge, J. Kyrouac, J. Schatz, Y. Zhang and S. Xie, 2015: The MC3E Sounding Network: Operations, Processing and Analysis. *Atmos. Meas. Tech.*, **8**,421-434, doi:10.5194/amt-8-1-2015.
- Klein, SA, and AD Del Genio. 2006. *ARM's Support for GCM Improvement: A White Paper*. U.S. Department of Energy. DOE/SC-ARM/P-06-012, Washington, D.C.
- 15 Kollias, P., B. A. Albrecht, E. E. Clothiaux, M. A. Miller, K. L. Johnson, and K. P. Moran (2005), The atmospheric radiation measurement program cloud profiling radars: An evaluation of signal processing and sampling strategies, *J. Atmos. Oceanic Technol.*, **22**, 930–948.
- 20 Kollias, P., M. A. Miller, K. L. Johnson, M. P. Jensen, and D. T. Troyan (2009), Cloud, thermodynamic, and precipitation observations in West Africa during 2006, *J. Geophys. Res.*, **114**, D00E08, doi:10.1029/2008JD010641.
- Kollias, P., et al. (2014), Scanning ARM cloud radars. Part II: Data quality control and processing, *J. Atmos. Oceanic Technol.*, **31**, 583–598.
- 25 Lamer, K., and P. Kollias (2015), Observations of fair-weather cumuli over land: Dynamical factors controlling cloud size and cover, *Geophys. Res. Lett.*, **42**, 8693–8701, doi:10.1002/2015GL064534.
- Lawson, R. P., D. O'Connor, P. Zmarzly, K. Weaver, B. Baker, and Q. Mo S, 2006: The 2D-S (Stereo) Probe: Design and Preliminary Tests of a New Airborne, High-Speed, High-Resolution Particle Imaging Probe. *J. Atmos. Oceanic Technol.*, **23**, 1462–1477, doi: 10.1175/JTECH1927.1.
- 30 Li, W., and R. Fu (2004), Transition of the large-scale atmospheric and land surface conditions from dry to wet season over Amazonia as diagnosed by the ECMWF Re-analysis, *J. Clim.*, **17**, 2637–2651.

- Liu, S. and X. Z. Liang (2010), Observed diurnal cycle climatology of planetary boundary layer height. *J. Clim.*, 23, 5790-5807.
- 5 Long, C. N., and T. P. Ackerman (2000), Identification of clear skies from broadband pyranometer measurements and calculation of downwelling shortwave cloud effects, *J. Geophys. Res.*, 105(D12), 15609–15626
- Long, C. N., and D. D. Turner (2008), A method for continuous estimation of clear-sky downwelling longwave radiative flux developed using ARM surface measurements, *J. Geophys. Res.*, 113, D18206, doi:10.1029/2008JD009936.
- 10 Long, C. N., J. H. Mather, and T. P. Ackerman, 2016: The ARM Tropical Western Pacific (TWP) sites. *The Atmospheric Radiation Measurement (ARM) Program: The First 20 Years, Meteor. Monogr.*, No. 57, Amer. Meteor. Soc.
- Malhi, Y., E. Pegoraro, A. D. Nobre, M. G. P. Pereira, J. Grace, A. D. Culf, and R. Clement, 2002: Energy and water dynamics of a central Amazonian rain forest. *J. Geophys. Res.*, 107, 8061, doi:10.1029/2001JD000623.
- 15 Marengo, J. A., Fisch, G. F., Alves, L. M., Sousa, N. V., Fu, R., and Zhuang, Y.: Meteorological context of the onset and end of the rainy season in Central Amazonia during the 2014–15 Go-Amazon Experiment, *Atmos. Chem. Phys. Discuss.*, doi:10.5194/acp-2017-22, in review, 2017.
- 20 Mather, J. H., 2005: Seasonal variability in clouds and radiation at the Manus ARM site. *J. Climate*, 18, 2417–2428,
- Mather, J.H., J. W. Voyles, 2013: The Arm Climate Research Facility: A Review of Structure and Capabilities. *Bull. Amer. Meteor. Soc.*, 94, 377–392.
- 25 Martin, S. T., Artaxo, P., Machado, L. A. T., Manzi, A. O., Souza, R. A. F., Schumacher, C., Wang, J., Andreae, M. O., Barbosa, H. M. J., Fan, J., Fisch, G., Goldstein, A. H., Guenther, A., Jimenez, J. L., Pöschl, U., Silva Dias, M. A., Smith, J. N., and Wendisch, M. 2016: Introduction: Observations and Modeling of the Green Ocean Amazon (GoAmazon2014/5), *Atmos. Chem. Phys.*, 16, 4785–4797, doi:10.5194/acp-16-4785-2016.
- 30 Martin, S. T., et al. (2017), The Green Ocean Amazon Experiment (GoAmazon2014/5) Observes Pollution Affecting Gases, Aerosols, Clouds, and Rainfall over the Rain Forest, *Bull. Am. Meteorol. Soc.*, doi:10.1175/BAMS-D-15-00221.1.

- Machado LAT, Laurent H, Dessay N, Miranda I. 2004. Seasonal and diurnal variability of precipitation over Amazon and its impact on convection over the Amazonia: A comparison of different vegetation types and large scale forcing. *Theor. Appl. Climatol.* 78: 61–77, DOI: 10.1007/s00704-004-0044-9.
- 5 May, P. T., and A. Ballinger, 2007: The statistical characteristics of convective cells in a monsoon regime (Darwin, Northern Australia). *Mon. Wea. Rev.*, **135**, 82–92,
- McFarlane, S. A., C. N. Long, and J. Flaherty (2013), A climatology of surface cloud radiative effects at the ARM tropical western Pacific sites, *J. Appl. Meteorol. Clim.*, 52 (4), 996–1013, doi:10.1175/Jame-D-12-0189.1.
- 10 Miller, M.A., K. Nitschke, T.P. Ackerman, W. Ferrell, N. Hickmon, and M. Ivey, 2014: The Atmospheric Radiation Measurement Mobile Facility, *Chapter, AMS Monograph, The first 20 years of ARM.*
- Minnis, P., et al. (2011), CERES Edition-2 cloud property retrievals using TRMM VIRS and Terra and Aqua MODIS data, Part I: Algorithms, *IEEE Trans. Geosci. Remote Sens.*, 49(11), 4374–4400.
- 15 Misra, V., 2008: Coupled air, sea, and land interactions of the South American monsoon. *J. Climate*, **21**, 6389–6403, doi:10.1175/2008JCLI2497.1.
- 20 Nobre, P., M. Malagutti, D.F. Urbano, R. A. F. De Almeida, and E. Giarolla (2009), Amazon deforestation and climate change in a coupled model simulation, *J. Clim.*, 22, 5686–5697.
- Nunes, A. M. P.; Silva Dias, M. A. F.; Anselmo, E. M.; Morales, C. A. 2016. Severe Convection Features in the Amazon Basin: A TRMM-Based 15-Year Evaluation. *Frontiers in Earth Science.*, v.4, 2016/000037.
- 25 Oliveria, A. P.; Fitzjarrald, D. R. The amazon river breeze and the local boundary layer: I. observations. *Boundary-Layer Meteorology*, Springer, v. 63, n. 1, p. 141 {162, 1993.
- Oue, M., P. Kollias, K. W. North, A. Tatarevic, S. Endo, A. M. Vogelmann, and W. I. Gustafson Jr. (2016), Estimation of cloud fraction profile in shallow convection using a scanning cloud radar, *Geophys. Res. Lett.*, 43, 10,998–11,006, doi:10.1002/2016GL070776.
- 30 Platnick, S., M. D. King, S. A. Ackerman, W. P. Menzel, B. A. Baum, J. C. Riédi, and R. A. Frey, 2003: The MODIS cloud products: Algorithms and examples from Terra. *IEEE Trans. Geosci. Remote Sens.*, 41, 459–473.

- Richter, I., and S. Xie, 2008: On the origin of equatorial Atlantic biases in coupled general circulation models. *Climate Dyn.*, **31**, 587.
- 5 Romatschke, U. and R. A. Houze Jr., 2010: Extreme Summer Convection in South America. *J. Climate*, **23**, 3761–3791. doi: <http://dx.doi.org/10.1175/2010JCLI3465.1>
- Rossow, W. B., G. Tselioudis, A. Polak, and C. Jakob (2005), Tropical climate described as a distribution of weather states indicated by distinct mesoscale cloud property mixtures, *Geophys. Res. Lett.*, **32**, L21812, doi:10.1029/2005GL024584.
- 10 Saraiva, I, MAF Silva Dias, CAR Morales, JMB Saraiva., Regional Variability of Rain Clouds in the Amazon Basin as Seen by a Network of Weather Radars, *Journal of Applied Meteorology and Climatology* **55** (12), 2657-2675, 2016
- Schiro, K. A., J. D. Neelin, D. K. Adams, and B. R. Linter, 2016: Deep convection and column water vapor over tropical land versus tropical ocean: A comparison between the Amazon and the tropical western Pacific. *J. Atmos. Sci.*, **73**, 4043–4063, doi:10.1175/JAS-D-16-0119.1.
- 15 Schiro, K. A.: Thermodynamic Controls on Deep Convection in the Tropics: Observations and Applications to Modeling, Ph.D. thesis, University of California, Los Angeles, Los Angeles, CA, 148 pp., 2017.
- 20 Schmid, B., R.G. Ellingson, and G.M. McFarquhar, 2016: ARM Aircraft Measurements, *The Atmospheric Radiation Measurement (ARM) Program: The First 20 Years*, *Meteor. Monogr.*, No. 57, Amer. Meteor. Soc.
- Silva Dias, M. A. F.; Dias, P. L. S.; Longo, M.; Fitzjarrald, D. R.; Denning, A. S. River breeze circulation in eastern amazonia: observations and modelling results. *Theoretical and Applied Climatology*, Springer, v. 78, n. 1-3, p. 111{121, 2004.
- 25 Steiner, M., R. A. Houze Jr., and S. Yuter, 1995: Climatological characterization of three-dimensional storm structure from operational radar and rain gauge data. *J. Appl. Meteor.*, **34**, 1978–2007, doi:10.1175/1520-30 0450(1995)034<1978:CCOTDS>2.0.CO;2.
- 30 Stokes, G. M. and S. E. Schwartz, 1994: The Atmospheric Radiation Measurement (ARM) Program: Programmatic background and design of the cloud and radiation test bed. *Bull. Amer. Meteor. Soc.*, **75**, 1201-1221.

- Tang, S., Xie, S., Zhang, Y., Zhang, M., Schumacher, C., Upton, H., Jensen, M. P., Johnson, K. L., Wang, M., Ahlgrim, M., Feng, Z., Minnis, P., and Thieman, M.: Large-scale vertical velocity, diabatic heating and drying profiles associated with seasonal and diurnal variations of convective systems observed in the GoAmazon2014/5 experiment, *Atmos. Chem. Phys.*, **16**, 14249–14264, doi:10.5194/acp-16-14249-2016, 2016.
- 5
- Thorsen, T. J., Q. Fu, J. M. Comstock, C. Sivaraman, M. A. Vaughan, D. M. Winker, and D. D. Turner, 2013: Macrophysical properties of tropical cirrus clouds from the CALIPSO satellite and from ground-based micropulse and Raman lidars. *J. Geophys. Res. Atmos.*, **118**, 9209–9220, doi:10.1002/jgrd.50691.
- 10
- Tridon, F., A. Battaglia, P. Kollias, E. Luke, and C. R. Williams (2013), Signal postprocessing and reflectivity calibration of the Atmospheric Radiation Measurement 915-MHz wind profilers, *J. Atmos. Oceanic Technol.*, **30**, 1038–1054.
- Twomey, S., 1974: Pollution and the Planetary Albedo. *Atmospheric Environment*, **8**, 1251–56.
- 15
- Wilkinson, J. M., R. J. Hogan, A. J. Illingworth, and A. Benedetti (2008), Use of a lidar forward model for global comparisons of cloud fraction between the ICESat lidar and the ECMWF model, *Mon. Weather Rev.*, **136**, 3742–3759.
- Williams, E., *et al.*, Contrasting convective regimes over the Amazon: Implications for cloud electrification, *J. Geophys. Res.*, **107**(D20), 8082, doi:10.1029/2001JD000380, 2002.
- 20
- Wu, W., Y. Liu, M. P. Jensen, T. Toto, M. J. Foster and C. N. Long, 2014: A comparison of multiscale variations of decade-long cloud fractions from six different platforms over the Southern Great Plains in the United States. *J. Geophys. Res.*, **119**, 3438–3459. Doi:10.1002/2013JD019813.
- 25
- Xie, S., R. T. Cederwall, and M. H. Zhang, 2004: Developing long-term single-column model/cloud system-resolving model forcing using numerical weather prediction products constrained by surface and top of the atmosphere observations. *J. Geophys. Res.*, **109**, D01104, doi:10.1029/2003JD004045.
- 30
- Xie, S., Y. Zhang, S. E. Giangrande, M. P. Jensen, R. McCoy, and M. Zhang (2014), Interactions between cumulus convection and its environment as revealed by the MC3E sounding array, *J. Geophys. Res. Atmos.*, **119**, 11,784–11,808, doi:10.1002/2014JD022011.
- Yin L, Fu R, Shevliakova E, Dickinson R., 2013; How well can CMIP5 simulate precipitation and its controlling processes over tropical South America? *Clim. Dyn.* **41**(11–12): 3127–3143, DOI: 10.1007/s00382-012-1582-y.

Zhang, M. and Lin, J., 1997: Constrained Variational Analysis of Sounding Data Based on Column-Integrated Budgets of Mass, Heat, Moisture, and Momentum: Approach and Application to ARM Measurements, *J. Atmos. Sci.*, 54, 1503–1524.

- 5 Zhuang, Y., R. Fu, J. A. Marengo, and H. Wang (2017), Seasonal variation of shallow-to-deep convection transition and its link to the environmental conditions over the Central Amazon, *J. Geophys. Res. Atmos.*, 122, doi:10.1002/2016JD025993.

Cloud type	Cloud-base height	Cloud-top height	Cloud thickness
Shallow	< 3 km	< 3 km	No restriction
Congestus	< 3 km	3-8 km	$\geq 1.5$ km
Deep convection	< 3 km	> 8 km	$\geq 5$ km
Alto cumulus	3-8 km	3-8 km	< 1.5 km
Alto stratus	3-8 km	3-8 km	$\geq 1.5$ km
Cirrostratus/anvil	3-8 km	> 8 km	$\geq 1.5$ km
Cirrus	> 8 km	> 8 km	No restriction

**Table 1.** Cloud-type definitions based on cloud boundaries and thickness. Definitions are slightly modified from Burleyson et al. [2015; their Table 2] and McFarlane et al. [2013; their Table 3].

		Mean frequency of cloud (%)	Mean frequency as the lowest cloud in column (%)	SW Trans (STD)	SW CRE ( $\text{W m}^{-2}$ )	LW CRE ( $\text{W m}^{-2}$ )
Low	All data	22.1	22.1	0.64 (0.28)	-177.5	17.7
	Wet seasons	27.9	27.9	0.60 (0.28)	-210.8	18.3
	Dry seasons	16.8	16.8	0.71 (0.27)	-132.5	15.1
Congestus	All data	5.7	4.8	0.36 (0.25)	-326.6	26.3
	Wet seasons	8.9	7.5	0.34 (0.23)	-346.3	25.5
	Dry seasons	2.8	2.4	0.40 (0.29)	-284.1	26.7
DeepConv.	All data	5.2	4.9	0.17 (0.15)	-425.9	28.4
	Wet seasons	9.0	8.4	0.18 (0.15)	-429.3	27.0
	Dry seasons	1.5	1.4	0.17 (0.16)	-487.6	33.4
Altoaccumulus	All data	19.6	13.6	0.73 (0.30)	-131.8	10.2
	Wet seasons	25.3	16.0	0.69 (0.30)	-153.4	10.1
	Dry seasons	14.9	11.6	0.79 (0.29)	-102.3	8.5
Altostratus	All data	1.9	1.0	0.52 (0.29)	-233.3	15.9
	Wet seasons	3.1	1.5	0.47 (0.25)	-252.0	14.9
	Dry seasons	0.8	0.4	0.57 (0.32)	-161.1	16.7
Cirrostratus	All data	7.6	4.2	0.50 (0.31)	-243.8	11.4
	Wet seasons	10.3	4.9	0.44 (0.25)	-296.9	12.4
	Dry seasons	4.2	2.6	0.61 (0.36)	-222.8	10.1
Cirrus	All data	29.7	17.2	0.79 (0.26)	-100.3	3.8
	Wet seasons	30.4	13.4	0.74 (0.28)	-121.2	3.8
	Dry seasons	24.9	18.0	0.85 (0.23)	-81.6	2.3

**Table 2:** Frequencies of cloud occurrence in the column and associated conditional SW transmissivity (SW Trans), conditional SW cloud radiative effect (SW CRE), and conditional LW cloud radiative effect (LW CRE) for each cloud type.

5 All values are averaged across the diurnal cycle. For SW CRE, only daytime hours are included. SW Transmissivity values in parentheses are standard deviations.

	SWdn	CSWdn	SW CRE	LWdn	CLWdn	LW CRE
Manaus (Central Amazonia)						
All data	197.5	291.9	-94.4	420.3	405.9	14.5
Wet seasons	<del>183.6</del>	<del>305.0</del>	<del>-121.5</del>	<del>423.7</del>	<del>405.9</del>	<del>17.8</del>
Dry seasons	<del>216.2</del>	<del>276.6</del>	<del>-60.4</del>	<del>415.0</del>	<del>404.9</del>	<del>10.1</del>
Darwin						
All data	232.4	293.4	-61.0	407.0	394.6	12.4
Wet seasons	226.5	321.5	-95.0	427.9	411.5	16.4
Dry seasons	239.1	262.7	-23.5	384.2	376.4	7.8
Manus						
All data	205.1	299.8	-94.7	423.5	408.2	15.3
Nauru						
All data	237.7	302.1	-64.4	420.6	408.5	12.2

- Deleted: 181.6
- Deleted: 297.1
- Deleted: -115.6
- Deleted: 423.5
- Deleted: 405.6
- Formatted Table
- Deleted: 17.8
- Deleted: 227.6
- Deleted: 282.5
- Deleted: -54.9
- Deleted: 414.4
- Deleted: 405.3
- Deleted: 9.1

**Table 3:** Mean downwelling SW radiative flux (SWdn), estimated clear-sky SW radiative flux (CSWdn), aggregate SW cloud radiative effect (SW CRE; SWdn - CSWdn), downwelling LW radiative flux (LWdn), estimated clear-sky LW radiative flux (CLWdn), aggregate LW cloud radiative effect (LW CRE; LWdn - CLWdn). All units are in W m<sup>-2</sup> and are averaged across the diurnal cycle. The Darwin, Manus, Nauru results are taken from Burleyson et al. (2015), Table 3.

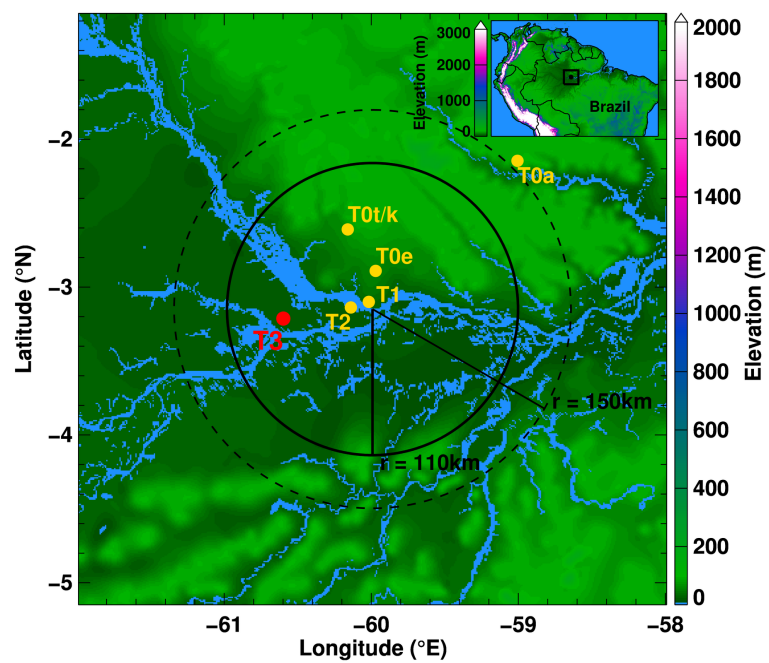
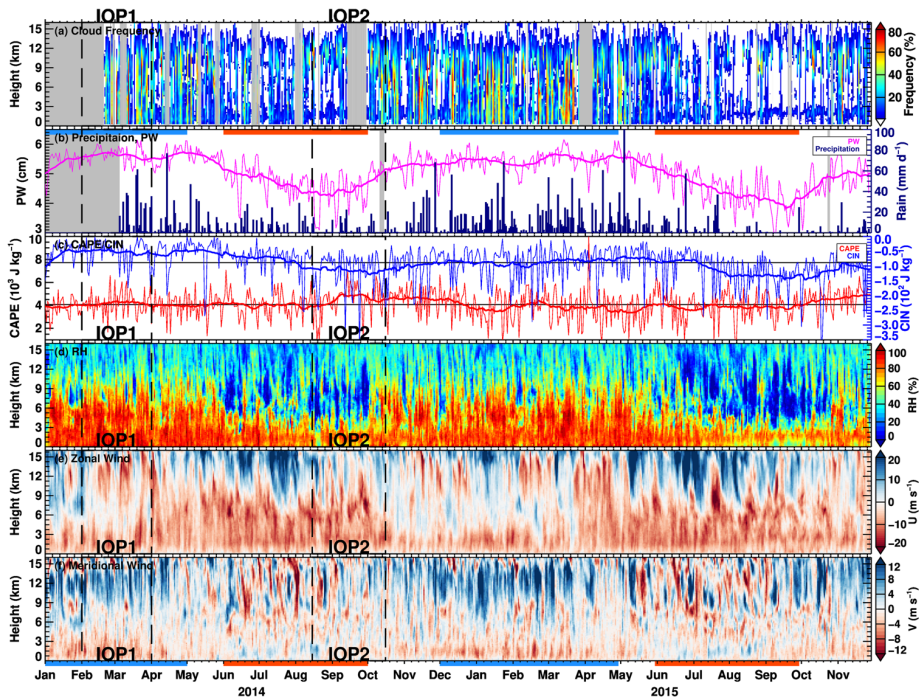


**Figure 1:** Location of the GoAmazon2014/5 key deployment sites and associated terrain elevation (shaded). The primary ARM AMF facilities were located at the T3 location. Range rings indicate distances from the SIPAM radar location near T1.

- 5 The 110 km range ring is the range associated with the ARM continuous forcing dataset domain.



5  
**Figure 2:** Time series of (a) cloud frequency from the merged WACR-ARSCL-RWP dataset, (b) column precipitable water (purple, thick line is 30-day running mean) and surface precipitation (dark blue bars), sounding measurements of (c) daily maximum CAPE (red), daily minimum CIN (blue), two horizontal lines are their respective mean values, (d) relative humidity (with respect to liquid), (e) zonal wind, and (f) meridional wind. The data shown are daily average values. Gray  
 10 fillings in (a,b) are periods with missing cloud or precipitation data, respectively. ‘Wet’ and ‘Dry’ seasons in this study are denoted with blue and orange bars in (b,f), IOP1 and IOP2 periods are denoted by the vertical dash lines.

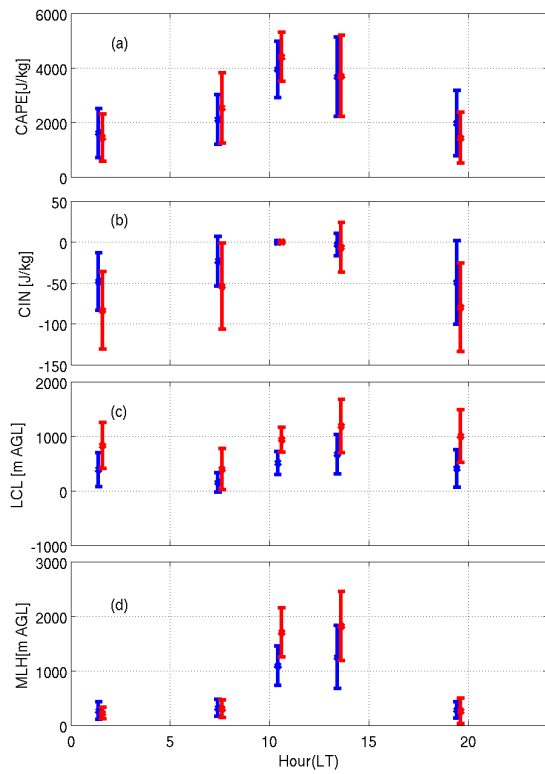


**Figure 3:** Diurnal cycles (mean and standard deviation) for radiosonde-based thermodynamic quantities of (a) CAPE, (b) CIN, (c) LCL height, and (d) MLH for wet (blue) and dry (red) season breakdowns.

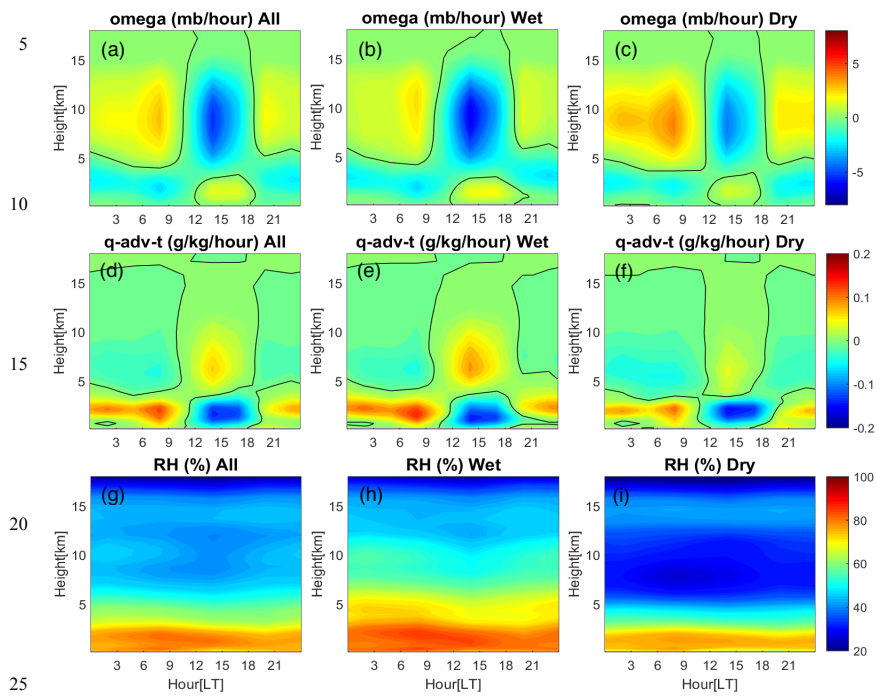


**Figure 4:** Diurnal cycles of omega, total advection of moisture and relative humidity (with respect to liquid) for the complete two-year GoAmazon2014/15 campaign record (left), as well as wet season (middle) and dry season (right) breakdowns.

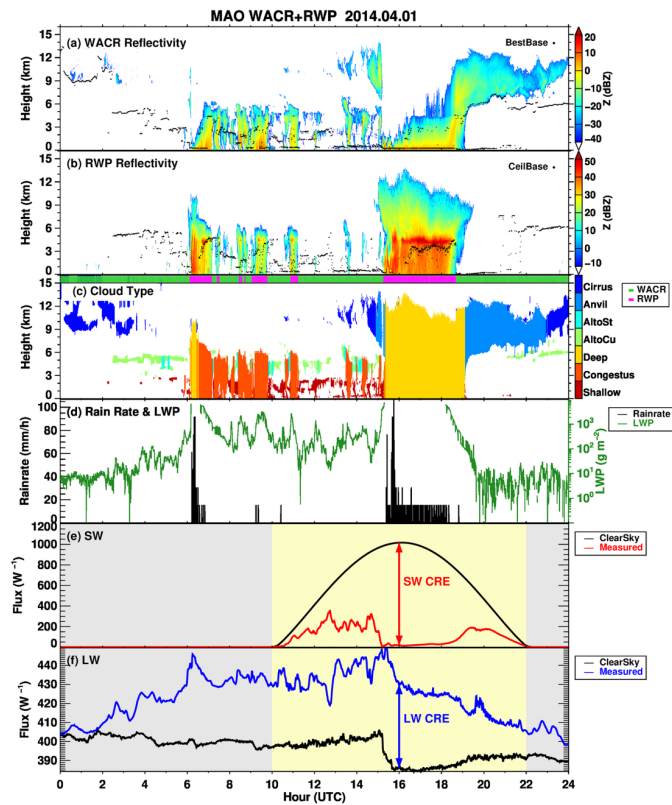


**Figure 5:** Example from the merged WACR-ARSCL-RWP dataset for a 1 April 2014 event: (a) WACR reflectivity, (b) RWP reflectivity, (c) cloud type classification, (d) tipping bucket rain rate (black, 5-minute increments) and MWR retrieved liquid water path (green), (e) downward shortwave flux, and (f) downward longwave flux. The black dots in panels (a,b) reflect a best estimate cloud-base height and ceilometer cloud-base height from the WACR-ARSCL dataset. Magenta color bars above (c) show periods when RWP data were used to replace WACR data (green color bars). The black lines in panels (e,f) reflect clear-sky flux estimates from the radiative flux analysis product. The difference between clear-sky estimated fluxes and measured fluxes (denoted between the arrows in e,f) are defined as cloud radiative effects.

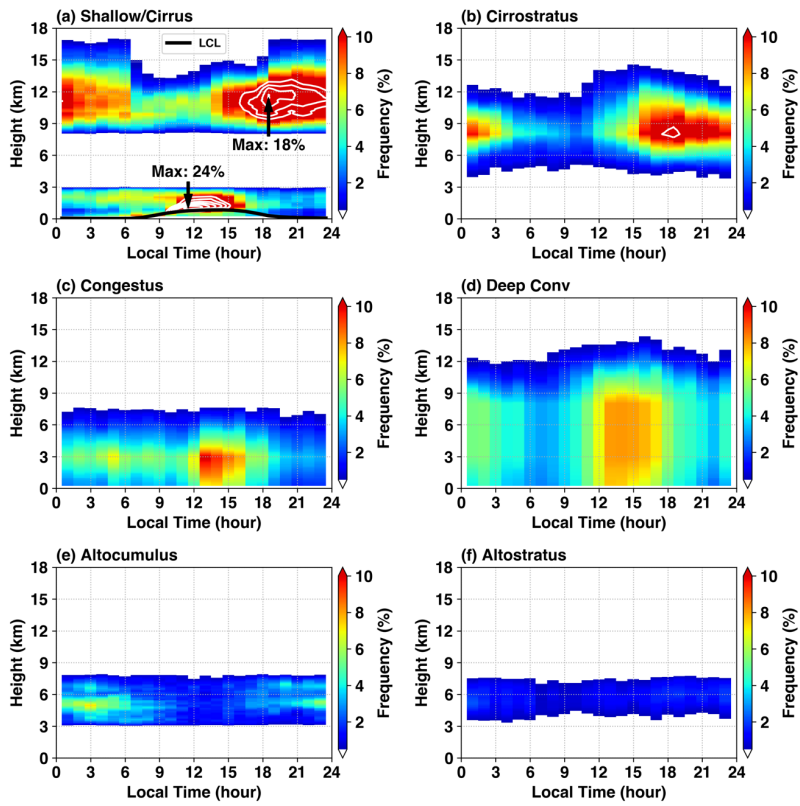
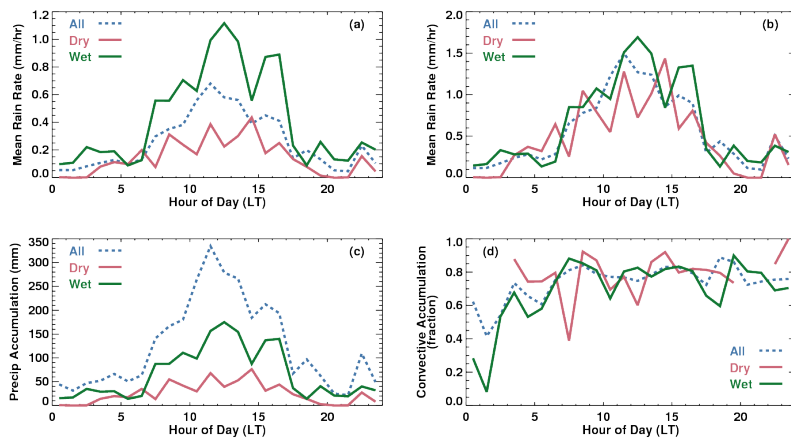


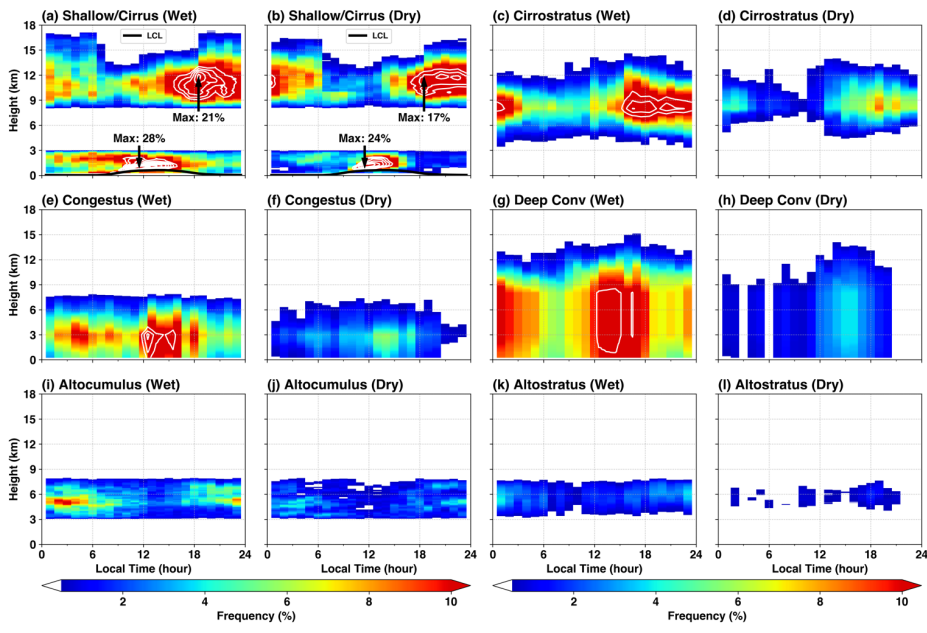
**Figure 6:** Composite diurnal cycle cloud fraction profiles segregated according to each of the seven cloud classification categories. White contours start at 10% and increment at 2%. Maximum cloud fraction values for shallow and cirrus clouds are marked in (a). The black line in (a) plots the averaged LCL height estimated using surface measurements.

5

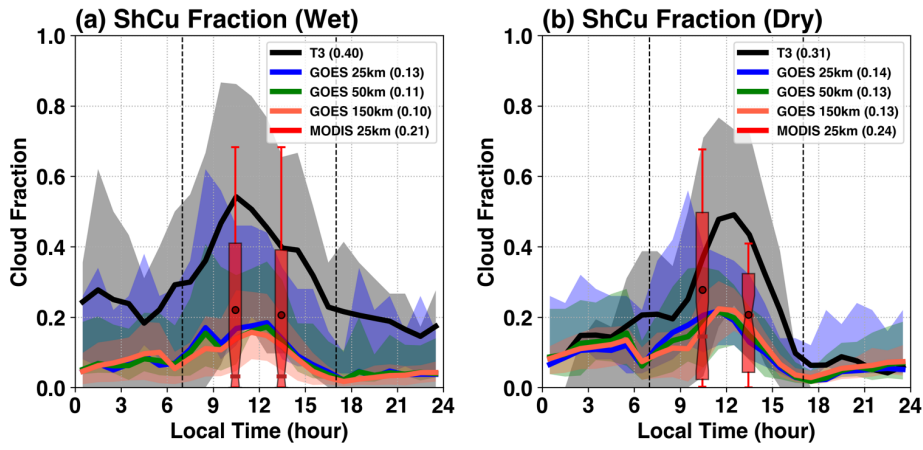


5 **Figure 7:** (a) Mean daily precipitation rate [mm hr<sup>-1</sup>] for all days, (b) for only the precipitating days during the campaign (> 1 mm), (c) the total accumulation in [mm] for the dataset and (d) the fractional convective accumulation as sampled by the rain gauges for summary campaign and associated wet and dry season conditions.

10



5 **Figure 8:** As in Fig. 6, but for wet season and dry season conditions.



10 **Figure 9:** Diurnal comparison of shallow cumulus (ShCu) cloud fraction estimates between ARM T3 (black lines and grey shading), MODIS (red box whisker) and GOES (multi-color, contingent on spatial domain) centered on the ARM T3 site for (a) wet and (b) dry season breakdowns during February – December 2014. Values in the legend reflect an averaged value during daytime (07 – 17 LT, vertical dash lines) hours. Shaded regions reflect the observational interquartile range. MODIS box-whisker notch shows median values, circle shows mean, box shows interquartile range, and whisker shows 10<sup>th</sup> and 90<sup>th</sup> percentiles, respectively.

**Formatted: Font:Bold**

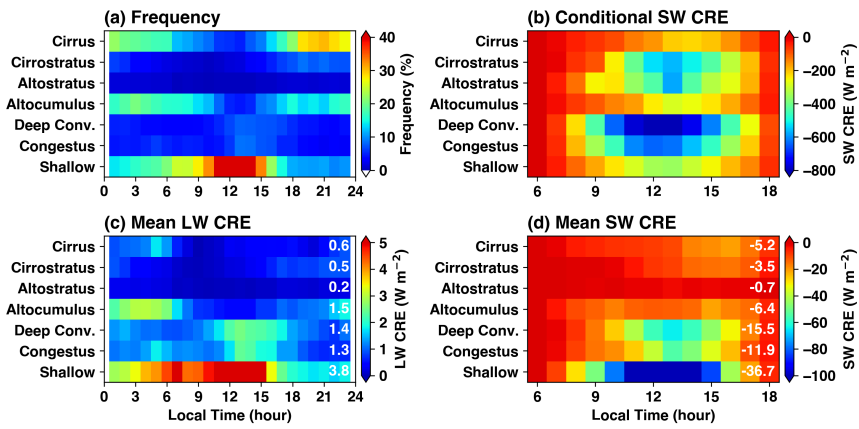
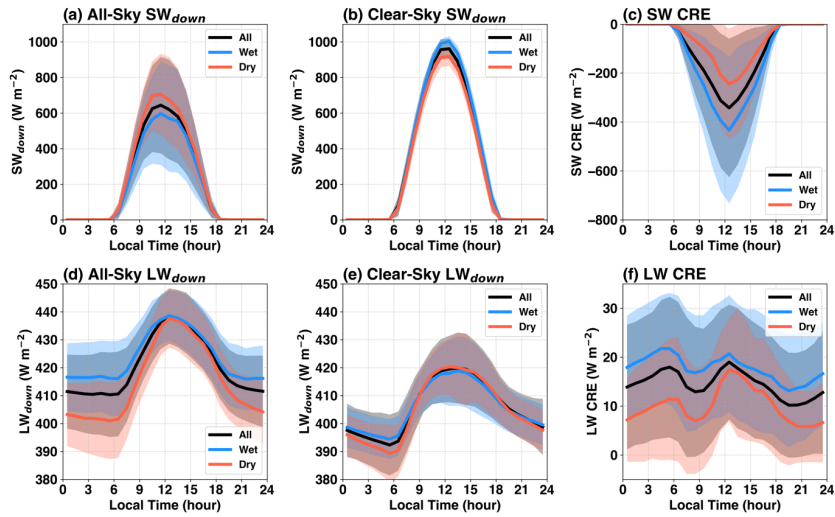
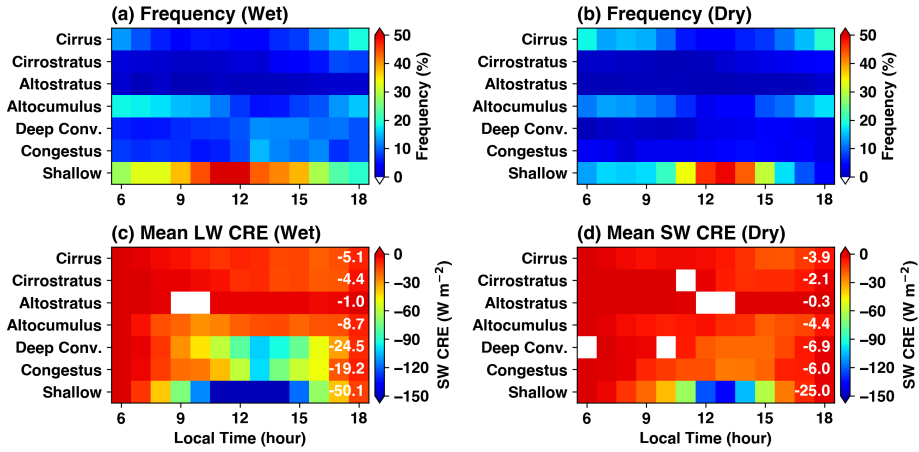


**Figure 10:** Mean cloud frequency and CRE for all GoAmazon2014/5 data. (a) Cloud frequency of occurrence as the lowest 10 cloud in the column as a function of the diurnal cycle (x axis), (b) conditional SW CRE, (c) mean LW CRE (frequency of occurrence times the conditional LW CRE), and (d) mean SW CRE (frequency of occurrence times the conditional SW CRE). Note (a,c) are for all hours and (b,d) are for daytime hours only. The white boxes are hours with insufficient data. The white numbers in (c,d) show the mean CRE values (in  $W m^{-2}$ ) averaged across the diurnal cycle (including nighttime).



5 **Figure 11:** As in Table 3, except with the full diurnal cycle for the (a) mean downwelling SW radiative flux, (b) estimated clear-sky SW radiative flux, (c) aggregate SW cloud radiative effects, (d) downwelling LW radiative flux, (e) estimated clear-sky LW radiative flux, and (f) aggregate LW cloud radiative effect. All units are in  $W m^{-2}$ . Shaded regions represent the observational standard deviation for these estimates during the hour.

10



5  
**Figure 12:** Wet (left column) and dry (right column) season comparisons for cloud frequency and SW CRE. (a,b) Cloud frequency of occurrence as the lowest cloud in the column, as a function of the diurnal cycle (x axis). (c,d) Mean SW CRE (frequency of occurrence times the conditional SW CRE). The white numbers in (c,d) [show the](#) mean CRE values (in  $W m^{-2}$ ) averaged across the diurnal cycle (including nighttime). The white boxes represent hours with insufficient data.

10

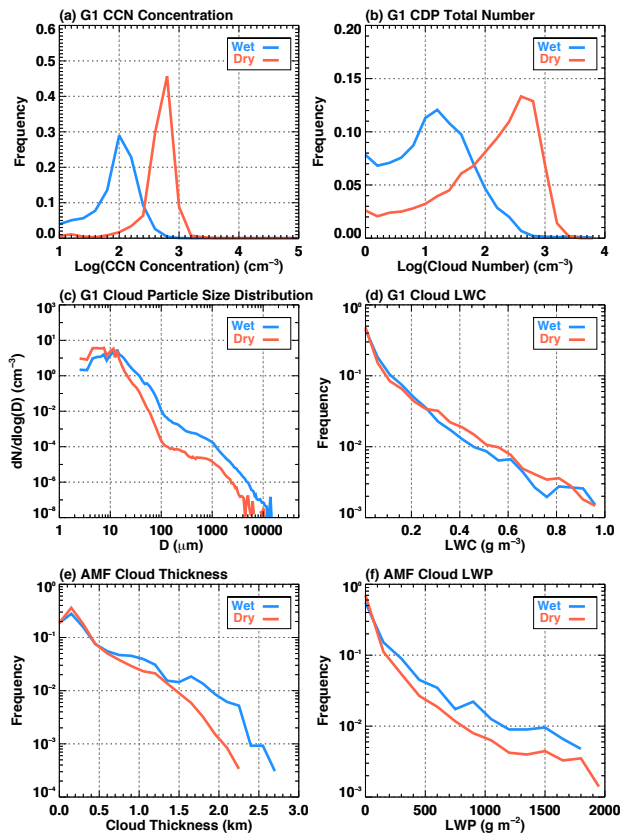


**Figure 13:** Shallow cumulus cloud micro- and macro-physics observed by AAF G1 aircraft and AMF surface instrumentation at the T3 site during the two IOPs in GoAmazon2014/5. (a) Cloud condensation nuclei number concentration, (b) cloud droplet total number concentration, (c) cloud particle size distribution, (d) cloud liquid water content (LWC), (e) cloud thickness, (f) cloud liquid water path (LWP).